Available online at www.sciencedirect.com
SCIENCE DIRECT®
Journal of Applied Geophysics 54 (2003) 219–246
JOURNAL OF APPLIED GEOPHYSICS
www.elsevier.com/locate/jappgeo

The acoustic signature of fluid flow in complex porous media ☆

Morten Jakobsen[a,*], Tor Arne Johansen[a], Clive McCann[b]

[a] University of Bergen, Department of Earth Science, Allegt. 41, Bergen N-5007 Norway
[b] University of Reading, Postgraduate Research Institute for Sedimentology, PO Box 227, Whiteknights, Reading, Berkshire, UK

Abstract

Effective medium approximations for the frequency-dependent and complex-valued effective stiffness tensors of cracked/porous rocks with multiple solid constituents are developed on the basis of the T-matrix approach (based on integral equation methods for quasi-static composites), the elastic–viscoelastic correspondence principle, and a unified treatment of the local and global flow mechanisms, which is consistent with the principle of fluid mass conservation. The main advantage of using the T-matrix approach, rather than the first-order approach of Eshelby or the second-order approach of Hudson, is that it produces physically plausible results even when the volume concentrations of inclusions or cavities are no longer small. The new formulae, which operates with an arbitrary homogeneous (anisotropic) reference medium and contains terms of all order in the volume concentrations of solid particles and communicating cavities, take explicitly account of inclusion shape and spatial distribution independently. We show analytically that an expansion of the T-matrix formulae to first order in the volume concentration of cavities (in agreement with the dilute estimate of Eshelby) has the correct dependence on the properties of the saturating fluid, in the sense that it is consistent with the Brown–Korringa relation, when the frequency is sufficiently low. We present numerical results for the (anisotropic) effective viscoelastic properties of a cracked permeable medium with finite storage porosity, indicating that the complete T-matrix formulae (including the higher-order terms) are generally consistent with the Brown–Korringa relation, at least if we assume the spatial distribution of cavities to be the same for all cavity pairs. We have found an efficient way to treat statistical correlations in the shapes and orientations of the communicating cavities, and also obtained a reasonable match between theoretical predictions (based on a dual porosity model for quartz–clay mixtures, involving relatively flat clay-related pores and more rounded quartz-related pores) and laboratory results for the ultrasonic velocity and attenuation spectra of a suite of typical reservoir rocks.

Keywords: Viscoelastic waves; Permeable composites; Finite concentrations; Pores; Cracks; Clay minerals

1. Introduction

The successful interpretation of acoustic (infrasonic, sonic, ultrasonic) data recorded on a wide variety of rocks may require a unified model, which accounts for the effects of microstructure and fluid flow on the overall wave characteristics. The present study represents a modest contribution to the development of such a model. It is based on the observation that

☆ This paper was presented at the 10th International Workshop on Seismic Anisotropy.

* Corresponding author. Tel.: +47-55-588359; fax: +47-55-589669.
E-mail addresses: morten@ifjf.uib.no (M. Jakobsen), torarne@ifjf.uib.no (T.A. Johansen), c.mccann@rdg.ac.uk (C. McCann).

0926-9851/$ - see front matter © 2003 Elsevier B.V. All rights reserved.
doi:10.1016/j.jappgeo.2002.11.004

rocks are generally composed of multiple solid constituents (crystals, minerals, fibres, fossils, etc.) and interconnected cavities (pores, cracks, fractures, channels, etc.), having a wide range of sizes, shapes, orientations, relative positions and number densities. We think that any theory for the macroscopic properties of rocks should have a strong stochastic component because randomness is one of the most prominent features of these materials. The cavities deserve particular attention because they represent the strongest heterogeneities and may be partially or completely saturated with a fluid (oil, gas, water, etc.) that may be of great practical interest to us. Because the fluid may flow from one cavity to another, or within a single cavity, when a macroscopic stress field is imposed on the system, the response of a single cavity may be time-dependent. The flow of fluid will lead to the dissipation of energy and so a single cavity may exhibit an elastic or effective viscoelastic behaviour. Many scientists (e.g., Klimentos and McCann, 1990; Best et al., 1994) have observed that, when an ultrasonic pulse propagates in a fluid-saturated porous/cracked rock, its amplitude will be attenuated and its shape will change because the different frequency components travel with different speeds. From Neumann's principle (e.g., Nowick, 1995), which states that any symmetry exhibited by the point group of the material must also be possessed by every physical property of the material, it is suggestive that velocities and attenuations may also depend on the direction of pulse propagation, if there exists alignments in the microstructure [though velocities and attenuations are (stochastic) wave characteristics rather than material properties]. Such anisotropy effects have in fact been observed in the laboratory (e.g., Jakobsen and Johansen, 1999, 2000; Domnesteanu et al., 2002). To make sense of it all, we propose that small deformations and waves in rocks should generally be analysed on the basis of linear (stochastic) model for viscoelastic, anisotropic composites.

Before we enter the complex realm of rocks as dynamic composites, let us note that it is customary to distinguish between two types of attenuation: namely, intrinsic attenuation (where acoustic energy is removed from the wave field by an elastic processes, such as those related to fluid flow) and apparent attenuation (where the acoustic energy is only redistributed to other parts of the wave field, by the multiple scattering of waves from heterogeneities in the medium). Both these types of acoustic attenuation cause a propagating acoustic pulse to loose energy (see Menke and Dubendorff, 1985), but it is only in the case of apparent attenuation that the total wave field energy is conserved. For an effective medium theory of composites like rocks, it is normally assumed that the wavelengths are very large compared with the scale of the microstructure, so that the apparent attenuation (associated with the multiple scattering of waves by the inclusions making up the composites) can safely be ignored. This assumption is not as restrictive as it appears since (the total) ultrasonic attenuation in vacuum dry rocks have been found to be negligible (see Tittmann, 1977). Although Klimentos and McCann (1990) speculated that grain scattering effects are responsible for a rapid rise in the observed attenuation coefficients as the frequency increases beyond 1 MHz or so, fluid flow is often believed to be the main source of acoustic attenuation in small rock samples (e.g., Biot, 1956a,b; Jones, 1986; Klimentos and McCann, 1990; Chapman et al., 2002). During the passage of an acoustic pulse, coherent movements of small fluid particles may occur at the macroscopic scale (Darcy flow) as well as on the microscopic scale (squirt flow). Darcy flow is a well-known phenomenon, and its effects on the overall wave characteristics can sometimes be described by the phenomenological theory of Biot (1956a,b), provided that the rock is composed of a single solid constituent and under high confining pressure with microcracks closed (see Klimentos and McCann, 1990; Best et al., 1994). The phenomenon of squirt flow is typically that fluid pressure is released from the more highly compressed flat cavities to the less compressed rounded cavities, with consequent effects on the overall wave speeds and attenuations, though the initial response of a fluid-saturated cavity under an imposed stress depends on its orientation as well as its shape. The effects of squirt flow are not included in the popular theory of Biot (1956a,b), and so it is not surprising that this theory has dramatically failed to explain the relatively high attenuation values we can observe in many rocks (that are assumed to be fully saturated with fluid and homogeneous on the macroscopic scale) containing cracks and/or other flat cavities

(see Jones, 1986; Chapman et al., 2002), often associated with multiple solid constituents (see Klimentos and McCann, 1990; Best et al., 1994). [A reviewer pointed out that relatively high attenuation levels may be obtained on the basis of a Biot-type of theory if we consider porous media that are partially saturated (e.g., Carcione et al., submitted for publication) and/or finely layered (e.g., Gurevich and Lopatnikov, 1995).]

Dvorkin and Nur (1993) have developed a unified model with the local and global flow mechanisms, which is [not consistent with the theory of Gassmann (1951), as it should be (see Thomsen, 1985), according to Chapman et al. (2002)] valid for porous media with a single solid constituent only and have another serious drawback in common with Biot's original model: microstructural information is simply incorporated through the use of empirically determined macroscopic parameters. In principle, it is possible to remove this drawback (see Burridge and Keller, 1981) and/or extend Biot's theory to complex porous media (see Berryman and Milton, 1991; Berryman, 1992, 1998; Berryman and Wang, 1998), but the works of many scientists (e.g., O'Connell and Budiansky, 1977; Budiansky and O'Connell, 1980; O'Connell, 1983; Hudson et al., 1996; Ravalec and Gueguen, 1996; Endres and Knight, 1997; Endres, 1997; Xu, 1998; Pointer et al., 2000; Jakobsen et al., 2000; Tod, 2001, 2002) suggest that a good theory for rocks need not necessarily be based on Biot's approach at all.

If the goal is to predict velocity and attenuation spectra in rocks as a function of their petrophysical parameters (or visa versa), as is may be for an application within seismic exploration or reservoir monitoring (e.g., Samec and Blangy, 1992; McCann et al., 1997; Koesoemadinata and McMechan, 2001), one should probably focus on inclusion-based models. Hudson et al. (1996), Pointer et al. (2000) and Tod (2001, 2002) have shown that progress along the inclusion-based line can be obtained if an extremely simple model of the porous microstructure is employed: namely, that where an anisotropic porous/permeable medium is containing a dilute concentration of small-aspect ratio spheroidal cracks that are distributed in space in accordance with an isotropic correlation function. Although the above theories based on Hudson's crack model are extremely interesting, there is an important need for a more general model that can deal with multiple solid constituents and interconnected cavities having a wider range of shapes, orientations, spatial distributions and number densities. Complexity is of course not a goal in itself but required by nature (e.g., Klimentos and McCann, 1990; Jakobsen and Johansen, 1999, 2000).

While we shall refer to Hudson et al. (1996) several times throughout the paper, we actually have in mind only the first part of that paper (dealing with connected cracks). The second part provided an equant porosity model, ostensibly to address the important storage porosity problem that has been the subject of other papers (e.g., Hudson et al., 2001). To provide an additional motivation for the present work (which deals with connected cracks and equant porosity in an unified manner), let us emphasize that the equant porosity model of Hudson et al. (1996) is not consistent with the (anisotropic Gassmann) Brown and Korringa (1975) relation, according to Chapman et al. (2002).

The outline of this paper is simple. First, we generalize the T-matrix theory of Jakobsen et al. (2003) to include the frequency-dependent effects of intercavity fluid flow. Then, we discuss some details for application, including those associated with possible statistical correlations in shapes and orientations of the cavities. Finally, we provide some numerical examples indicating the power and flexibility of the more general T-matrix approach. Specifically, we discuss the concept of crack-induced anisotropy, and use the new theory to match ultrasonic velocity and attenuation measurements on clayey sandstones.

2. The T-matrix approach to rock physics

2.1. General considerations

There exists a variety of theoretical methods that can be used attack the many-body problem in rock physics and seismic reservoir characterization; that is, to estimate the overall properties of a heterogeneous material. Among the more interesting ones are the method of smoothing (e.g., Hudson, 1980, 1981; 1994a,b; Jakobsen et al., 2000), the variational method (e.g., Willis, 1981; Ponte Castaneda and Willis, 1995) and the T-matrix approach (e.g., Zeller and

Dederich, 1973; Domany et al., 1975; Nan et al., 1998; Jakobsen et al., 2003).The choice of a particular method may not only depend on the problem at hand but also on the experience of the worker. Some of us find the T-matrix approach particularly attractive because it is based on physically transparent integral equation methods (Green's function techniques) similar to those used in quantum scattering theory, and gives physically plausible results even when the inclusion concentrations are no longer very small. The importance of the problem of inclusions at finite concentration is discussed by Molinari and Mouden (1996).

Before we start to become more and more technical, let us briefly outline the physical significance and advantage of the T-matrix approach used in this study. This follows naturally if we note that Jakobsen et al. (2003) derived an exact solution for the effective stiffness tensor of a micro-inhomogeneous medium in terms of a fourth-rank tensor field **T**, which (can be represented by a 6×6 T-matrix, for example if we use the Kelvin notation of Appendix A) completely determines the (transitions out of the homogeneous strain state associated with the arbitrary homogeneous reference medium) strain field at all points within a representative volume. The highly developed iterative or perturbative methods of modern physics can be used in rock physics because the T-matrix of a solid earth material satisfies a Lippmann–Schwinger type of integral equation, similar to the central equation of quantum mechanical scattering or many-body theory.

Jakobsen et al. (2003) showed that the T-matrix for a general class of inclusion-based models can be written exactly as an infinite series involving an increasing number of t-matrices (taking into account the interactions between all points within a single inclusion in an exact manner) and other terms (associated with the interaction between points located in different inclusions). Jakobsen et al. (2003) assumed that the net interactions between different inclusions are small in some sense and truncated the series expansion for the T-matrix of the material after the second-order term involving two t-matrices only, in order to avoid facing a difficult three-body problem that can hardly be solved analytically.

As first emphasized by Zeller and Dederich (1973), 'second order' in the perturbation series for the T-matrix of the material does not mean 'second order' in the perturbation series for the effective stiffness tensor, in the sense that a T-matrix approximation for the effective stiffnesses based on two-point statistics may contain terms of all order in the volume concentrations of inclusions, in contrast with the approximations of Hudson (1980, 1981, 1994a,b) based on the method of smoothing.

Following Jakobsen et al. (2003), we consider a unified model for media with inclusions that are either embedded in a homogeneous matrix material or else make up a granular aggregate. The population of inclusions is divided into families of inclusions having the same shape/orientation, t-matrices $\mathbf{t}^{(n)}$ (defined below in terms of stiffness fluctuations) and volume concentration $v^{(n)}$, labelled by $n = 1,2,\ldots,N$. The term inclusion is used generically and may not only denote a solid particle (crystal, mineral, basic building block, etc.) but also a cavity (pore, crack, fracture, channel, etc.) that may or may not be filled with fluid (liquid, gas). The effective stiffness tensor $\mathbf{C}^*$ is given by (Jakobsen et al., 2003)

$$\mathbf{C}^* = \mathbf{C}^{(0)} + \mathbf{C}_1 : (\mathbf{I}_4 + \mathbf{C}_1^{-1} : \mathbf{C}_2)^{-1}, \tag{1}$$

$$\mathbf{C}_1 = \sum_{r=1}^{N} v^{(r)} \mathbf{t}^{(r)}, \tag{2}$$

$$\mathbf{C}_2 = \sum_{r=1}^{N} \sum_{s=1}^{N} v^{(r)} \mathbf{t}^{(r)} : \mathbf{G}_{\mathrm{d}}^{(rs)} : \mathbf{t}^{(s)} v^{(s)}. \tag{3}$$

Here $\mathbf{C}^{(0)}$ is the stiffness tensor for a homogeneous reference medium, which can be (anisotropic) selected rather arbitrary without violating the mechanical stability criterium (see Auld, 1990); $\mathbf{I}_4$ is the identity for fourth-rank tensors (which can be represented by the 6×6 unit matrix); $\mathbf{G}_{\mathrm{d}}^{(rs)}$ is given by the strain Green's function (for a material with properties given by $\mathbf{C}^{(0)}$) integrated over a characteristic *ellipsoid* having the same aspect ratio as $p^{(s|r)}(\mathbf{x} - \mathbf{x}')$, which, in turn, gives the probability density for finding an inclusion of type s at point $\mathbf{x}'$ given that there is an inclusion of type r at point $\mathbf{x}$. The t-matrix for a single inclusion of type n is given by (Zeller and Dederich, 1973; Jakobsen et al., 2003)

$$\mathbf{t}^{(n)} = (\mathbf{C}^{(n)} - \mathbf{C}^{(0)}) : [\mathbf{I}_4 - \mathbf{G}^{(n)} : (\mathbf{C}^{(n)} - \mathbf{C}^{(0)})]^{-1}, \tag{4}$$

where $\mathbf{G}^{(n)}$ is a fourth-rank tensor depending only on $\mathbf{C}^{(0)}$ and the shape/orientation of the nth inclusion type. The $\mathbf{G}^{(n)}$ tensor can in principle be evaluated for inclusions having any shape/orientation (see Appendix C), but we assume normally that the inclusions are ellipsoidal in shape, so that the $\mathbf{G}^{(n)}$ tensors are given by an integral over a finite range. (The expression for the $\mathbf{G}^{(n)}$ tensor for an ellipsoidal inclusion can also be used to evaluate the $\mathbf{G}_{\mathrm{d}}^{(rs)}$ tensor, provided that the aspect ratio of the correlation function is taken to be identical with that of the associated inclusion.)

2.2. The physical significance of the t-matrix

The t-matrix $\mathbf{t}^{(n)}$ for a single inclusion of type n may be regarded as a kind of renormalized stiffness fluctuation $(\mathbf{C}^{(n)}-\mathbf{C}^{(0)})$ (see Zeller and Dederich, 1973; McCoy, 1979; Jakobsen et al., 2003). To clarify its physical interpretation, let us note that the strain $\boldsymbol{\epsilon}^{(n)}$ within a single inclusion of type n and the uniform applied strain $\boldsymbol{\epsilon}^{(0)}$ at infinity are related by (Zeller and Dederich, 1973; Korringa, 1979; Jakobsen et al., 2003)

$$(\mathbf{C}^{(n)}-\mathbf{C}^{(0)}):\boldsymbol{\epsilon}^{(n)}=\mathbf{t}^{(n)}:\boldsymbol{\epsilon}^{(0)}. \tag{5}$$

Setting

$$\boldsymbol{\epsilon}^{(0)}=\mathbf{S}^{(0)}:\boldsymbol{\sigma}^{(0)}, \tag{6}$$

where $\boldsymbol{\sigma}^{(0)}$ is the applied stress corresponding with the strain $\boldsymbol{\epsilon}^{(0)}$, we get

$$\boldsymbol{\epsilon}^{(n)}=\mathbf{K}^{(n)}:\boldsymbol{\sigma}^{(0)}, \tag{7}$$

where

$$(\mathbf{C}^{(n)}-\mathbf{C}^{(0)}):\mathbf{K}^{(n)}=\mathbf{t}^{(n)}:\mathbf{S}^{(0)}. \tag{8}$$

Combining Eqs. (4) and (8), we get

$$\mathbf{K}^{(n)}=[\mathbf{I}_4-\mathbf{G}^{(n)}:(\mathbf{C}^{(n)}-\mathbf{C}^{(0)})]^{-1}:\mathbf{S}^{(0)}, \tag{9}$$

which agree with the result of Hornby et al. (1994). The above results were originally obtained under the assumption that we are dealing with purely elastic inclusions. If n represents an anisotropic mineral, then we normally know what to use for $\mathbf{C}^{(n)}$. If n represents a fully fluid-saturated cavity that is isolated with respect to fluid flow, then $\mathbf{C}^{(n)}$ is simply related to the bulk modulus of the saturating fluid. If n represents a dry cavity, then we may set $\mathbf{C}^{(n)}=0$, since a dry cavity may formally be regarded as an elastic continuum having vanishing stiffnesses (e.g., Nemat-Nasser and Hori, 1993; Ponte Castaneda and Willis, 1995; Xu, 1998). If n represents a communicating cavity, that is, a fully fluid-saturated cavity, which is allowed to exchange fluid mass with other cavities, due to local and/or global pressure gradients (caused by the passage of a long acoustic wave), then we do not immediately know what to use for $\mathbf{C}^{(n)}$, but, from Eqs. (8) and (9), we get

$$\mathbf{t}^{(n)}=(\mathbf{G}^{(n)})^{-1}:(\mathbf{K}^{(n)}:\mathbf{C}^{(0)}-\mathbf{I}_4), \tag{10}$$

which means that we can find the t-matrix for a communicating cavity provided that we know the corresponding K-matrix. This is an agreeable feature because the K-matrix can be found from the superposition of results from two different ‘gedanken’ experiments involving both the dry and saturated version of the cavity, as shown in Section 2.3.

Realizing that the response of some of the inclusions within a rock-like composite may be viscoelastic does not lead to an intractable problem, since the solution of a viscoelastic problem can (under proper circumstances, involving sufficiently low frequencies) be obtained from the solution of the corresponding elastic problem by appealing to the correspondence principle (e.g., O’Connell and Budiansky, 1977; Budiansky and O’Connell, 1980; Willis, 1981; Brinson and Lin, 1998; Dunn, 1995; Brinson and Lin, 1998; Gibiansky and Torquato, 1998), and replacing the (real-valued and frequency-independent) elastic moduli in the elastic solution by the corresponding (complex-value and frequency-dependent) viscoelastic moduli.

2.3. The t-matrix for a communicating cavity

The population of inclusions making up a rock-like composite may generally be divided into N_{c} sets of cavities and N_{s} sets of solid particles; that is, one may always write $N=N_{\mathrm{c}}+N_{\mathrm{s}}$. Without any loss of generality, one may assume that the nth inclusion set consist of cavities if $1<n\leq N_{\mathrm{c}}$ and solid particles if $N_{\mathrm{c}}<n\leq N$. We have already discussed how to evalu-

ate the t-matrices of various solid particles and cavities that are isolated with respect to fluid flow. The goal of the present section is to include the effects of fluid flow. Therefore, we shall assume that $1 < n \leq N_c$, so that we are indeed dealing with a communicating cavity.

By linear superposition (see Mukerji and Mavko, 1994), the strain inside a cavity of type n that is completely saturated with fluid under pressure $p_f^{(n)}$, under the imposed stress $\boldsymbol{\sigma}^{(0)}$ at infinity, is given by the strain within the corresponding dry cavity under the imposed stress $(\boldsymbol{\sigma}^{(0)} + \mathbf{I}_2 p_f^{(n)})$ minus the strain within a similarly shaped and oriented cavity with hydrostatic stress $\mathbf{I}_2 p_f^{(n)}$ applied both at infinity and inside the cavity, where $\mathbf{I}_2$ is the identity for second-rank tensors (which can be represented by the 3×3 unit matrix). If we use this argument in conjunction with Eqs. (7) and (9), we get

$$\mathbf{K}^{(n)} : \boldsymbol{\sigma}^{(0)} = \mathbf{K}_d^{(n)} : (\boldsymbol{\sigma}^{(0)} + \mathbf{I}_2 p_f^{(n)}) - \mathbf{S}^{(0)} : \mathbf{I}_2 p_f^{(n)}, \quad (11)$$

where

$$\mathbf{K}_d^{(n)} = (\mathbf{I}_4 + \mathbf{G}^{(n)} : \mathbf{C}^{(0)})^{-1} : \mathbf{S}^{(0)}, \quad (12)$$

is the K-matrix of a dry cavity of type n. Eq. (12) is consistent with (the observation that dry cavities can formally be treated as inclusions having vanishing stiffnesses) Eq. (9).

From the linearity of our problem, we know that there exists a second-rank tensor $\boldsymbol{\psi}^{(n)}$, which relates the fluid pressure in the nth cavity set to the applied stress; that is,

$$p_f^{(n)} = \boldsymbol{\psi}^{(n)} : \boldsymbol{\sigma}^{(0)}. \quad (13)$$

By using Eqs. (11) and (13) in conjunction with the fact that $\boldsymbol{\sigma}^{(0)}$ is arbitrary, we find that

$$\mathbf{K}^{(n)} = \mathbf{K}_d^{(n)} + (\mathbf{K}_d^{(n)} - \mathbf{S}^{(0)}) : (\mathbf{I}_2 \otimes \boldsymbol{\psi}^{(n)}), \quad (14)$$

where the symbol $\otimes$ denotes the dyadic tensor product and means that

$$(\mathbf{I}_2 \otimes \boldsymbol{\psi}^{(n)})_{ijkl} = \delta_{ij} (\boldsymbol{\psi}^{(n)})_{kl}. \quad (15)$$

If we insert the expression (14) for $\mathbf{K}^{(n)}$ into the expression (10) for $\mathbf{t}^{(n)}$, we get

$$\mathbf{t}^{(n)} = \mathbf{t}_d^{(n)} + (\mathbf{G}^{(n)})^{-1} : (\mathbf{K}_d^{(n)} - \mathbf{S}^{(0)}) : (\mathbf{I}_2 \otimes \boldsymbol{\psi}^{(n)}) : \mathbf{C}^{(0)}, \quad (16)$$

where

$$\mathbf{t}_d^{(n)} = (\mathbf{G}^{(n)})^{-1} : (\mathbf{K}_d^{(n)} : \mathbf{C}^{(0)} - \mathbf{I}_4). \quad (17)$$

Since Eq. (17) imply that

$$\mathbf{t}_d^{(n)} : \mathbf{S}^{(0)} = (\mathbf{G}^{(n)})^{-1} : (\mathbf{K}_d^{(n)} - \mathbf{S}^{(0)}), \quad (18)$$

we can write Eq. (17) more elegantly as

$$\mathbf{t}^{(n)} = \mathbf{t}_d^{(n)} + \mathbf{t}_d^{(n)} : \mathbf{S}^{(0)} : (\mathbf{I}_2 \otimes \boldsymbol{\psi}^{(n)}) : \mathbf{C}^{(0)}. \quad (19)$$

By inserting the expression (12) for $\mathbf{K}_d^{(n)}$ into Eq. (17) for $\mathbf{t}_d^{(n)}$, we see that

$$\mathbf{t}_d^{(n)} = -\mathbf{C}^{(0)} : (\mathbf{I}_4 + \mathbf{G}^{(n)} : \mathbf{C}^{(0)})^{-1}, \quad (20)$$

which is consistent with Eq. (4). Thus, the problem has been reduced to the evaluation of $\boldsymbol{\psi}^{(n)}$, which is the cavity fluid pressure polarization tensor in our vocabulary.

To find $\boldsymbol{\psi}^{(n)}$ in the case of a communicating cavity, we obviously need to introduce elements of fluid dynamics. If $\tilde{v}^{(n)}$ and $\rho_f^{(n)}$ is the porosity and density of the nth cavity set, respectively, then the total fluid mass m_f is given by

$$m_f = \sum_{r=1}^{N_c} \tilde{v}^{(r)} \rho_f^{(r)}. \quad (21)$$

Since our theory allows for finite concentrations of arbitrarily shaped cavities, the total fluid mass does not have to be very small. This is in contrast with the theory of Hudson et al. (1996), where the analogous expression for the total fluid mass involves only the very small volume of fluid one can expect to find inside a small number of very thin cracks. In other words, Hudson et al. (1996) did not include the essential storage porosity in their fluid dynamical considerations, like we do in the present study.

Following Hudson et al. (1996), we now require that the fluid mass in an arbitrary volume is conserved

and that the average flow of fluid is regulated by Darcy's law. This means that

$$\frac{\partial m_{\mathrm{f}}}{\partial t} = \nabla \cdot \left(\frac{\rho_{\mathrm{f}}}{\eta_{\mathrm{f}}} \mathbf{\Gamma} \cdot \nabla p_{\mathrm{f}} \right), \tag{22}$$

where p_{f} is the average (local) fluid pressure, ρ_{f} is the fluid mass density, η_{f} is the viscosity of the fluid and $\mathbf{\Gamma}$ is a second-rank tensor of permeability parameters. If the permeability tensor is isotropic, then the above equation reduces to that derived by Hudson et al. (1996). More generally, the above expression accounts for the fact that fluid may flow easier in some directions than others, depending on the degree of alignment in the microstructure. The tensor $\mathbf{\Gamma}$ represents the overall permeability of the material (including all cavities) and is assumed to be spatially invariant. For later reference, let us note that the fluid pressure and density of the nth cavity set are related by (Hudson et al., 1996)

$$\frac{\rho_0}{\rho_{\mathrm{f}}^{(n)}} = 1 - \frac{p_{\mathrm{f}}^{(n)}}{\kappa_{\mathrm{f}}}, \tag{23}$$

where ρ_0 is the density of the unstressed fluid and κ_{f} is the fluid bulk modulus. If a quasi-static stress field is imposed on the macroscopic specimen, then the pressure $p_{\mathrm{f}}^{(n)}$ in the fluid changes, due both to a change in porosity and to fluid flow. From Eqs. (7) and (11), we find the following first-order expression for the change in porosity:

$$\frac{\tilde{\nu}^{(n)} - \nu^{(n)}}{\nu^{(n)}} = (K_{\mathrm{d}}^{(n)})_{uupq}(\sigma_{pq}^{(0)} + \delta_{pq} p_f^{(n)}) - S_{uupq}^{(0)} \delta_{pq} p_{\mathrm{f}}^{(n)}, \tag{24}$$

where $\nu^{(n)}$ is the unstressed porosity of the nth cavity set. We assume that the mass flow out of the nth set of cavities is controlled by an expression similar to that of Hudson et al. (1996):

$$\frac{\partial (\rho_{\mathrm{f}}^{(n)} \tilde{\nu}^{(n)})}{\partial t} = -\frac{\nu^{(n)} \rho_0}{\kappa_{\mathrm{f}} \tau} (p_{\mathrm{f}}^{(n)} - p_{\mathrm{f}}), \tag{25}$$

where τ is a (squirt flow) relaxation time constant that can be estimated for the kind of microstructures studied by Hudson et al. (1996) and otherwise needs to be determined empirically. The analysis of Hudson et al. (1996) suggests that τ is normally proportional to the fluid viscosity η_{f} and sometimes inversely proportional to a permeability constant. If τ is proportional to the viscosity η_{f}, then our final results will be functions of the product $\omega\eta_{\mathrm{f}}$, in agreement with the observations of Jones (1986). An interesting justification for the use of an ansatz like that in Eq. (25) (was recently provided by Hudson) can be found in an appendix to the paper of Tod (2001). We have assumed that τ is independent of the shape/orientation index n, but it is only the implementation of the theory which becomes more difficult if we relax on this assumption, that may or may not be a good one (see O'Connell and Budiansky, 1977; Chapman et al., 2002). The analysis of Chapman (2002) suggests that τ is dependent on the scale-size (or surface area) of the cavity, suggesting that the present theory can easily be extended to model fractured porous/cracked media under the assumption that the scale-size of the fractures is much larger than that of the pores/cracks. We shall however (assume that the cavities we are dealing with have roughly the same scale-size) use the ansatz (25) in the present study, though we realize that there may perhaps be a need for further work on the development of local flow models. A comparison of theoretical predictions and experimental observations may also be useful in this connection.

We now introduce a second-rank tensor ψ, which relates the average fluid pressure and applied stress by

$$p_{\mathrm{f}} = \psi : \boldsymbol{\sigma}^{(0)}. \tag{26}$$

Assuming that the propagating plane wave has frequency ω, we find from Eq. (23) that

$$\psi^{(n)} = \frac{\psi - i\omega\tau\kappa_{\mathrm{f}} \mathbf{I_2} : \mathbf{K_d^{(n)}}}{1 + i\omega\gamma^{(n)}\tau}, \tag{27}$$

$$\gamma^{(n)} = 1 + \kappa_{\mathrm{f}}(K_{\mathrm{d}}^{(n)} - S^{(0)})_{uuvv}, \tag{28}$$

to first order in $p_{\mathrm{f}}^{(n)}/\kappa_{\mathrm{f}}$ and $(\tilde{\nu}^{(n)} - \nu^{(n)})/\nu^{(n)}$. To find the ψ tensor for substitution into Eq. (27), we first derive an expression for m_{f} by combining Eqs. (21) and (24). We then substitute for $p_{\mathrm{f}}^{(n)}$ in terms of p_{f} and $\boldsymbol{\sigma}^{(0)}$ by using Eqs. (13), (26) and (27). The resulting expression for m_{f} is inserted into a Fourier representation of the evolution law (22); we replace the

operators $\partial/\partial t$ and $\partial/\partial x_i$ with $i\omega$ and $-ik_i$, respectively, where k_i is a component of the wave number vector $\mathbf{k}$. Since the intermediate calculations at this point are quite similar to those described in the paper of Hudson et al. (1996), we give here only the final result for ψ:

$$\psi = -\Theta(\Sigma_a, \Sigma_b) \sum_{r=1}^{N_c} \frac{v^{(r)} \mathbf{I}_2 : \mathbf{K}_d^{(r)}}{1 + i\omega\gamma^{(r)}\tau}, \tag{29}$$

$$\Theta(\Sigma_a, \Sigma_b) = \kappa_f \left\{ \left(1 - \kappa_f S^{(0)}_{uuvv}\right)\Sigma_a + \kappa_f \Sigma_b - \frac{ik_u k_v \Gamma_{uv} \kappa_f}{\eta_f \omega} \right\}^{-1}, \tag{30}$$

$$\Sigma_a = \sum_{r=1}^{N_c} \frac{v^{(r)}}{1 + i\omega\gamma^{(r)}\tau}, \tag{31}$$

$$\Sigma_b = \sum_{r=1}^{N_c} \frac{v^{(r)} (K_d^{(r)})_{uuvv}}{1 + i\omega\gamma^{(r)}\tau}. \tag{32}$$

By using Eqs. (19), (27) and (29), we find that

$$\mathbf{t}^{(n)} = \mathbf{t}_d^{(n)} + \frac{\Theta(\Sigma_a, \Sigma_b)\mathbf{Z}^{(n)} + i\omega\tau\kappa_f \mathbf{X}^{(n)}}{1 + i\omega\gamma^{(n)}\tau}, \tag{33}$$

where

$$\mathbf{X}^{(n)} = -\mathbf{t}_d^{(n)} : \mathbf{S}^{(0)} : (\mathbf{I}_2 \otimes \mathbf{I}_2) : \mathbf{K}_d^{(n)} : \mathbf{C}^{(0)}, \tag{34}$$

and

$$\mathbf{Z}^{(n)} = -\mathbf{t}_d^{(n)} : \mathbf{S}^{(0)} : (\mathbf{I}_2 \otimes \mathbf{I}_2) : \left(\sum_{r=1}^{N_c} \frac{v^{(r)} \mathbf{K}_d^{(r)}}{1 + i\omega\gamma^{(r)}\tau} \right) : \mathbf{C}^{(0)}. \tag{35}$$

It is clear from Eqs. (12) and (20) that

$$\mathbf{K}_d^{(n)} : \mathbf{C}^{(0)} = -\mathbf{S}^{(0)} : \mathbf{t}_d^{(n)}. \tag{36}$$

Thus, we may also write Eqs. (34) and (35) in terms of $\mathbf{t}_d^{(n)}$ as

$$\mathbf{X}^{(n)} = \mathbf{t}_d^{(n)} : \mathbf{S}^{(0)} : (\mathbf{I}_2 \otimes \mathbf{I}_2) : \mathbf{S}^{(0)} : \mathbf{t}_d^{(n)}, \tag{37}$$

and

$$\mathbf{Z}^{(n)} = \mathbf{t}_d^{(n)} : \mathbf{S}^{(0)} : (\mathbf{I}_2 \otimes \mathbf{I}_2) : \mathbf{S}^{(0)} : \left(\sum_{r=1}^{N_c} \frac{v^{(r)} \mathbf{t}_d^{(r)}}{1 + i\omega\gamma^{(r)}\tau} \right), \tag{38}$$

respectively.

3. Some details for application

3.1. On the replacement of summation with integration

Summation over inclusions can, for computational convenience, be replaced by multiple integration over inclusion shapes and orientations. (The inclusion size may also be relevant, but not if we ignore scattering attenuation and accept the ansatz (25) for the mass flow out of a single cavity). This is the continuous limit used by Shafiro and Kachanov (1997) and others. Tod (2001), for example, did his calculations in this continuous limit, but assumed that the shapes and orientations of the flat cracks he was dealing with were independent on each other. [More realistically, one can expect the shape of a crack to depend upon its orientation relative to an applied anisotropic stress field (Tod, 2002).]

Alternatively, one may continue to sum over the inclusion shapes but integrate over inclusion orientations. This is the quasi-continuous limit used by Gubernatis and Krumhansl (1975) and others. Jakobsen et al. (2002), for example, calculated the effective elastic constants of anisotropic composites like shales in this quasi-continuous limit, by assigning a separate orientation distribution function to each shape factor.

If the goal is to make rapid progress in the general case, where it may not only be required to account for statistical correlations in the inclusion shapes and orientations but also to account for the effects of spatial correlations, then it is probably a good idea to stick to the quasi-continuous limit. The quasi-continuous limit offers an adequate theoretical platform for dealing with real rocks characterized by a discrete spectrum of cavity aspect ratios with multiple (and widely separated) peaks in the broad interval separating a perfectly spherical pore from a typical flat Hudson-crack (e.g., Cheng and Toksoz, 1979; O'Connell, 1983; Ravalec and Gueguen, 1996).

To summarize the above, we shall assume we are dealing with a continuous spectrum of cavity orientations but a discrete spectrum of cavity aspect ratios or shape factors. In the spirit of Cheng and Toksoz (1979), we re-divide the population of cavities into new sets of cavities, each set (labelled by $j=1,\ldots,J_c$) characterized by a common aspect ratio $\alpha^{(j)}$, porosity $\phi^{(j)}$ and orientation distribution function $O^{(j)}(\Omega)$. For any quantity $\mathbf{A}^{(r)}$ depending on the orientation/shape index r, we may let

$$\sum_{r=1}^{N_c} v^{(r)}\mathbf{A}^{(r)} \rightarrow \sum_{j=1}^{J_c} \phi^{(j)}\bar{\mathbf{A}}^{(j)}, \tag{39}$$

where

$$\bar{\mathbf{A}}^{(j)} = \int \mathrm{d}\,\Omega O^{(j)}(\Omega)\mathbf{A}(\alpha^{(j)},\Omega), \tag{40}$$

represents the orientation average of $\mathbf{A}(\alpha^{(j)}, \Omega)$ and Ω symbolizes the three Euler angles (see Jakobsen et al., 2003) determining the orientation of the cavity relative to the crystallographic axes of the material with properties given by $\mathbf{C}^{(0)}$. To get the normalization correct, we ensure that

$$\sum_{j=1}^{J_c} \phi^{(j)} = \sum_{r=1}^{N_c} v^{(r)}, \tag{41}$$

and

$$\int \mathrm{d}\Omega\; O^{(j)}(\Omega) = 1. \tag{42}$$

Without any loss of generality, we may always write the formula for the first-order correction as

$$\mathrm{C}_1 = \sum_{j=1}^{J_c} \phi^{(j)}\bar{\mathbf{t}}^{(j)}, \tag{43}$$

but the corresponding formula for the second-order correction;

$$\mathbf{C}_2 = \sum_{j=1}^{J_c}\sum_{k=1}^{J_c} \phi^{(j)}\bar{\mathbf{t}}^{(j)} : \bar{\mathrm{G}}_{\mathrm{d}}^{(jk)} : \phi^{(k)}\bar{\mathbf{t}}^{(k)}, \tag{44}$$

is only valid if the spatial distribution of cavities is independent of the orientations (as we assume in the following). In Eq. (44), we have introduced the tensor $\bar{\mathbf{G}}_{\mathrm{d}}^{(jk)}$, which is given by the usual expression for the $\mathbf{G}$ tensor of an ellipsoidal inclusion (Appendix C), provided that the aspect ratio of the associated inclusion is set equal to $\alpha_{\mathrm{d}}^{(jk)}$, which, in turn, is the aspect ratio of the characteristic ellipsoid determining the symmetry of the (translation invariant) conditional probability density $\bar{p}^{(k|j)}(\mathbf{x}-\mathbf{x}')$ for finding a cavity with aspect ratio $\alpha^{(k)}$ centred at point $\mathbf{x}'$ given that there is an cavity with aspect ratio $\alpha^{(j)}$ centred at point $\mathbf{x}$, independent of the cavity orientations. It remains to derive an expression for the orientation average of the t-matrix for a single communicating cavity.

3.2. On the use of isotropic reference media

The theory does not require that $\mathbf{C}^{(0)}$ is isotropic, but the analysis becomes much simpler if we assume that this is indeed the case. To see this, let us start with an evaluation of the γ factors. From Eqs. (28) and (12), we get

$$\gamma(\alpha^{(j)},\Omega) = 1 + \kappa_{\mathrm{f}}[K_{\mathrm{d}}(\alpha^{(j)},\Omega) - S^{(0)}]_{uuvv}, \tag{45}$$

and

$$\mathbf{K}_{\mathrm{d}}(\alpha^{(j)},\Omega) = [\mathbf{I}_4 + \mathbf{G}(\alpha^{(j)},\Omega) : \mathbf{C}^{(0)}]^{-1} : \mathbf{S}^{(0)}, \tag{46}$$

respectively.

Since $\mathbf{K}_{\mathrm{d}}$ must obey the usual transformation law for fourth-rank tensors, we can always write

$$\mathbf{K}_{\mathrm{d}}(\alpha^{(j)},\Omega) = \mathbf{R}(\Omega)::[\mathbf{K}_{\mathrm{d}}(\alpha^{(j)},\Omega)]^{\mathrm{local}}, \tag{47}$$

where $[\mathbf{K}_{\mathrm{d}}(\alpha^{(j)}, \Omega)]^{\mathrm{local}}$ refers to the value of $\mathbf{K}_{\mathrm{d}}(\alpha^{(j)}, \Omega)$ in the local coordinate system with axes coinciding with the principal axes of the nth type of ellipsoidal cavities;

$$[\mathbf{K}_{\mathrm{d}}(\alpha^{(j)},\Omega)]^{\mathrm{local}} = \{\mathbf{I}_4 + [\mathbf{G}(\alpha^{(j)},\Omega)]^{\mathrm{local}} : (\mathbf{C}^{(0)})^{\mathrm{local}}\}^{-1} : (\mathbf{S}^{(0)})^{local}, \tag{48}$$

and

$$\mathbf{R}(\Omega) = \mathbf{a}(\Omega)\otimes\mathbf{a}(\Omega)\otimes\mathbf{a}(\Omega)\otimes\mathbf{a}(\Omega), \tag{49}$$

where $\mathbf{a}(\Omega)$ is a transformation tensor function of Ω, which satisfies the following orthogonality relation (see Jeffreys and Jeffreys, 1972):

$$\mathbf{a}(\Omega)\cdot\mathbf{a}(\Omega)=\mathbf{I}_2. \tag{50}$$

However, we need to assume that $\mathbf{C}^{(0)}$ is isotropic to ensure that

$$[\mathbf{G}(\alpha^{(j)},\Omega)]^{\text{local}}=\mathbf{G}(\alpha^{(j)},\mathbf{0}), \tag{51}$$

(cf. Mura, 1982), which implies that

$$[\mathbf{K}_{\text{d}}(\alpha^{(j)},\Omega)]^{\text{local}}=\mathbf{K}_{\text{d}}(\alpha^{(j)},\mathbf{0}), \tag{52}$$

due to the relationship between $\mathbf{G}$ and $\mathbf{K}_{\text{d}}$ in Eq. (46). When we combine the above result with the transformation relation (47) and the orthogonality relation (50), we get

$$[K_{\text{d}}(\alpha^{(j)},\Omega)]_{uuvv}=[K_{\text{d}}(\alpha^{(j)},\mathbf{0})]_{uuvv}, \tag{53}$$

which implies that

$$\gamma(\alpha^{(j)},\Omega)=\gamma(\alpha^{(j)},\mathbf{0})\equiv\gamma_j, \tag{54}$$

since γ is defined as shown in Eq. (45). The above relation means that the γ factor for a cavity that may have any shape is independent of its orientations. This agrees with the findings of Hudson et al. (1996), which were only valid for flat cavities or cracks.

From the expression (33) for the t-matrix of a single communicating cavity, and Eq. (54) for γ, we get

$$\bar{\mathbf{t}}^{(j)}=\bar{\mathbf{t}}_{\text{d}}^{(j)}+\frac{\Theta(\Sigma_a,\Sigma_b)\bar{\mathbf{Z}}^{(j)}+i\omega\tau\kappa_{\text{f}}\bar{\mathbf{X}}^{(j)}}{1+i\omega\gamma_j\tau}. \tag{55}$$

If we impose the rule (39) on the expressions (38), (31), (32) [and also use Eq. (53) in connection with Σ_b], we get

$$\bar{\mathbf{Z}}^{(j)}=\bar{\mathbf{t}}_{\text{d}}^{(j)}:\mathbf{S}^{(0)}:(\mathbf{I}_2\otimes\mathbf{I}_2):\mathbf{S}^{(0)}:\left(\sum_{j=1}^{J_{\text{c}}}\frac{\phi^{(j)}\bar{\mathbf{t}}_{\text{d}}^{(j)}}{1+i\omega\gamma_j\tau}\right), \tag{56}$$

$$\Sigma_a=\sum_{j=1}^{J_{\text{c}}}\frac{\phi^{(j)}}{1+i\omega\gamma_j\tau}, \tag{57}$$

$$\Sigma_b=\sum_{j=1}^{J_{\text{c}}}\frac{\phi^{(j)}[K_{\text{d}}(\alpha^{(j)},\mathbf{0})]_{uuvv}}{1+i\omega\gamma_j\tau}, \tag{58}$$

respectively. Thus, we have reduced a rather complicated problem to the averaging of the fourth-rank tensors $\mathbf{t}_{\text{d}}$ and $\mathbf{X}$ using a separate orientation distribution function for each aspect ratio or shape factor, labelled by $j=1,\ldots,J_{\text{c}}$.

3.3. Evaluation of $\bar{\mathbf{t}}_d^{(j)}$

From Eq. (20), we get

$$\mathbf{t}_{\text{d}}(\alpha^{(j)},\Omega)=-\mathbf{C}^{(0)}:[\mathbf{I}_4+\mathbf{G}(\alpha^{(j)},\Omega):\mathbf{C}^{(0)}]^{-1}. \tag{59}$$

Since we have assumed $\mathbf{C}^{(0)}$ to be isotropic, it follows that

$$\mathbf{t}_{\text{d}}(\alpha^{(j)},\Omega)=\mathbf{R}(\Omega):\mathbf{t}_{\text{d}}(\alpha^{(j)},\mathbf{0}), \tag{60}$$

(cf. Eq. 51), which means that

$$\bar{\mathbf{t}}_{\text{d}}^{(j)}=\bar{\mathbf{R}}^{(j)}:\mathbf{t}_{\text{d}}(\alpha^{(j)},\mathbf{0}), \tag{61}$$

where

$$\bar{\mathbf{R}}^{(j)}=\int \text{d}\Omega\; O^{(j)}(\Omega)\mathbf{R}(\Omega), \tag{62}$$

represents an averaging operator or tensor of eight rank. Since t-matrix satisfies the same symmetry relations as the elastic stiffness tensor; namely,

$$(t_{\text{d}})_{ijkl}=(t_{\text{d}})_{jikl}=(t_{\text{d}})_{ijlk}=(t_{\text{d}})_{klij}, \tag{63}$$

it follows that we can find the orientation average of $\mathbf{t}_{\text{d}}(\alpha^{(j)},\ \Omega)$ in the same way as Morris (1969) and Sayers (1994) found that of the elastic stiffness tensor.

Following the above workers, we now specify $\Omega=(\xi,\ \phi,\ \psi)$ where θ, ϕ and ψ are three Eulerian angles and $\xi=\cos\theta$; and expand $O^{(j)}(\Omega)$ in terms of spherical harmonics:

$$O^{(j)}(\xi,\phi,\psi)=\sum_{l=0}^{\infty}\sum_{m=-l}^{l}\sum_{n=-l}^{l}W_{lmn}^{(j)}Z_{lmn}(\xi)\text{e}^{-im\phi}\text{e}^{-in\psi}, \tag{64}$$

where Z_{lmn} is a generalized Legendre function and

$$W_{lmn}^{(j)} = \frac{1}{4\pi^2}\int_0^{2\pi} d\psi \int_0^{2\pi} d\phi \times \int_{-1}^{1} d\xi\ O^{(j)}(\xi,\phi,\psi) Z_{lmn}(\xi) e^{im\phi} e^{in\psi}. \quad (65)$$

Since the t-matrix is actually a tensor of fourth rank, its orientation average depends only on the coefficients $W_{lmn}^{(j)}$ of the expansion of $O^{(j)}(\xi, \phi, \psi)$ for $l \le 4$. If the orientation distribution is symmetric about the axis $\theta = 0$, then $O^{(j)}$ is a function of ξ only and all the parameters $W_{lmn}^{(j)}$ are zero unless $m = n = 0$. [The assumption of axial symmetry is not strictly required, since Sayers (1994) also considered media with orthorhombic symmetry.] In addition, $O^{(j)}(\xi) = O^{(j)}(-\xi)$ and so $W_{l00}^{(j)}$ is zero unless l is even. The formulae for the $W_{l00}^{(j)}$ are fairly simple, e.g.,

$$W_{200}^{(j)} = \sqrt{\frac{5}{2}}\int_{-1}^{1} d\xi\ O^{(j)}(\xi) P_2(\xi), \quad (66)$$

$$W_{400}^{(j)} = \sqrt{\frac{9}{2}}\int_{-1}^{1} d\xi\ O^{(j)}(\xi) P_4(\xi), \quad (67)$$

where $P_n(\xi)$ is the Legendre polynomial of order n.

It follows from the work of Sayers (1994) that the components $\bar{t}_{IJ}^{(j)}$ and $t_{IJ}^{(j)}(\mathbf{0})$ $(I,J = 1,2,3,4,5,6)$ of $\bar{\mathbf{t}}_{\mathrm{d}}^{(j)}$ and $\mathbf{t}_{\mathrm{d}}(\alpha^{(j)}, \mathbf{0})$, respectively, are (in the notation of Kelvin) related by

$$\bar{t}_{11}^{(j)} = \bar{t}_{22}^{(j)} = \lambda^{(j)} + 2\mu^{(j)} + \frac{4\sqrt{2}}{105}\pi^2 \times [2\sqrt{5}a_3^{(j)} W_{200}^{(j)} + 3a_1^{(j)} W_{400}^{(j)}], \quad (68)$$

$$\bar{t}_{33}^{(j)} = \lambda^{(j)} + 2\mu^{(j)} - \frac{16\sqrt{2}}{105}\pi^2 \times [\sqrt{5}a_3^{(j)} W_{200}^{(j)} - 2a_1^{(j)} W_{400}^{(j)}], \quad (69)$$

$$\bar{t}_{12}^{(j)} = \lambda^{(j)} - \frac{4\sqrt{2}}{315}\pi^2 \times [2\sqrt{5}(7a_2^{(j)} - a_3^{(j)}) W_{200}^{(j)} - 3a_1^{(j)} W_{400}^{(j)}], \quad (70)$$

$$\bar{t}_{13}^{(j)} = \bar{t}_{23}^{(j)} = \lambda^{(j)} + \frac{4\sqrt{2}}{315}\pi^2 \times [\sqrt{5}(7a_2^{(j)} - a_3^{(j)}) W_{200}^{(j)} - 12a_1^{(j)} W_{400}^{(j)}], \quad (71)$$

$$\bar{t}_{55}^{(j)} = \bar{t}_{44}^{(j)} = \mu^{(j)} - \frac{2\sqrt{2}}{315}\pi^2 \times [\sqrt{5}(7a_2^{(j)} + 2a_3^{(j)}) W_{200}^{(j)} + 24a_1^{(j)} W_{400}^{(j)}], \quad (72)$$

$$\bar{t}_{66}^{(j)} = (\bar{t}_{11}^{(j)} - \bar{t}_{12}^{(j)}), \quad (73)$$

where

$$15\lambda^{(j)} = t_{11}^{(j)}(\mathbf{0}) + t_{33}^{(j)}(\mathbf{0}) + 5t_{12}^{(j)}(\mathbf{0}) + 8t_{13}^{(j)}(\mathbf{0}) - 8t_{55}^{(j)}(\mathbf{0}), \quad (74)$$

$$30\mu^{(j)} = 7t_{11}^{(j)}(\mathbf{0}) + 2t_{33}^{(j)}(\mathbf{0}) - 5t_{12}^{(j)}(\mathbf{0}) - 4t_{13}^{(j)}(\mathbf{0}) + 24t_{55}^{(j)}(\mathbf{0}). \quad (75)$$

and

$$a_1^{(j)} = t_{11}^{(j)}(\mathbf{0}) + t_{33}^{(j)}(\mathbf{0}) - 2t_{13}^{(j)}(\mathbf{0}) - 8t_{55}^{(j)}(\mathbf{0}), \quad (76)$$

$$a_2^{(j)} = t_{11}^{(j)}(\mathbf{0}) - 3t_{12}^{(j)}(\mathbf{0}) + 2t_{13}^{(j)}(\mathbf{0}) - 4t_{55}^{(j)}(\mathbf{0}), \quad (77)$$

$$a_3^{(j)} = 4t_{11}^{(j)}(\mathbf{0}) - 3t_{33}^{(j)}(\mathbf{0}) - t_{13}^{(j)}(\mathbf{0}) - 4t_{55}^{(j)}(\mathbf{0}). \quad (78)$$

Here, $\lambda^{(j)}$ and $\mu^{(j)}$ represent the isotropic part of the fourth-rank tensor $\bar{\mathbf{t}}^{(j)}$, while $a_i^{(j)}$ $(i = 1,2,3)$ represents the anisotropic part. The isotropic part of a tensor is per definition invariant under symmetry transformations belonging to the SO(3) group. Group theory is commonly used in other parts of physics to make sense of the internal symmetries of a complex system.

3.4. Evaluation of $\bar{\mathbf{X}}^{(j)}$

From Eq. (37), we get

$$\mathbf{X}(\alpha^{(j)}, \Omega) = \mathbf{t}_{\mathrm{d}}(\alpha^{(j)}, \Omega) : \mathbf{S}^{(0)} : (\mathbf{I}_2 \otimes \mathbf{I}_2) : \mathbf{S}^{(0)} : \mathbf{t}_{\mathrm{d}}(\alpha^{(j)}, \Omega). \quad (79)$$

Since we have assumed $\mathbf{C}^{(0)}$ to be isotropic, it follows from Eqs. (60) and (79) that

$$\mathbf{X}(\alpha^{(j)}, \Omega) = \mathbf{R}(\Omega) :: \mathbf{X}(\alpha^{(j)}, 0), \tag{80}$$

which means that

$$\bar{\mathbf{X}}^{(j)} = \bar{\mathbf{R}}^{(j)} :: \mathbf{X}(\alpha^{(j)}, 0). \tag{81}$$

It is clear from the structure of Eq. (79) and the symmetries of $\mathbf{t}_d$ in Eq. (63) that

$$X_{ijkl} = X_{jikl} = X_{ijlk} = X_{klij}. \tag{82}$$

All these mean that we can find the orientation average of the **X**-tensor in the same way as we found that of the $\mathbf{t}_d$-tensor, that is, by using the analytical results of Sayers (1994).

4. Numerical examples and discussion

4.1. Crack-induced anisotropy

Crack-induced anisotropy is of extreme importance in a large number of geophysical applications ranging from earthquake prediction to petroleum and geothermal exploration (Cheng, 1993). The 10th International Workshop on Seismic Anisotropy has left us with the impressions that the concept of shear wave splitting though a cracked or fractured medium is still being regarded as a useful diagnostic of such a medium. Until quite recently, the commonly used crack-induced anisotropy model was that of Hudson (1980, 1981), which is limited to a special class of microstructures with isotropic two-point correlation functions for the statistics of the distributions of centers of flat cracks (Douma, 1988; Hudson, 1994a) at dilute concentrations (Cheng, 1993), which are not only embedded in an isotropic matrix material (Hudson, 1994b) but also isolated with respect to fluid flow (Thomsen, 1995). In the generalization of Hudson's original crack model provided by Hudson et al. (1996), the cracks are no longer isolated with respect to fluid flow, but the important storage porosity was partially ignored in the fluid dynamical considerations, and we still have these other assumptions that restrict the range of applicability of the theory.

With the introduction of the T-matrix approach to rock physics, we can now deal with a more general class of microstructures with anisotropic two-point correlation functions for the statistics of the distributions of centers of arbitrarily shaped inclusions or cavities at finite concentration; in a way that involves the use of an arbitrary (anisotropic) reference medium and takes into account the storage porosity in the fluid dynamical equations. Tod (2001) writes that the model of connected cracks proposed by Hudson et al. (1996) for the transfer of fluid between cracks by non-compliant pores makes the assumption that the distortion of the pores is negligible compared with that of the cracks during the passage of a wave and that the porosity is low, so that we neglect compression of the pore fluid. Clearly, this is a rather restrictive assumption that has now been 'partially' removed in the process of developing a unified theory of rocks as viscoelastic composites. By 'partially' we mean that there are plenty of rooms of alternative solutions, depending on the assumptions one make about the relative length-scale-sizes of the cracks and the pores, among other things.

The T-matrix approach is quite general but needs to be adapted to reflect the microstructures of real rocks as seen in the laboratory or in the field. To illustrate that there has been a kind of progress, we shall soon investigate the effects of various non-trivial crack distributions on the overall properties of a dual porosity medium, involving a mixture of spherical pores and flat pores that are randomly oriented. But first we need establish what happens to such a medium when the crack density is zero, so that we have a useful reference for comparison. In order to mimic the behaviour of something like a sandstone, we let $\mathbf{C}^{(0)}$ represent the elastic stiffness constants of pure quartz (Table 1). The

Table 1
Mechanical properties of selected rock components

Component	ρ (kg/m^3)	c_{11} (GPa)	c_{33} (GPa)	c_{55} (GPa)	c_{66} (GPa)	c_{13} (GPa)
Quartz	2650	9.70	9.70	4.43	4.43	8.34
Clay	2520	17.15	5.26	1.48	6.63	2.71
Water	1000	2.20	2.20	0.00	0.00	2.20

The values we have used for the mass densities and elastic moduli (in the notation of Voigt) for the fluid and solid components were taken from the papers of Jakobsen et al. (2000) and Sams and Andrea (2001), respectively.

pore shape aspect ratios of the uncracked medium are given by $\alpha^{(1)}=1$ and $\alpha^{(2)}=0.05$, and we use $\phi^{(1)}=0.2094$ and $\phi^{(2)}=0.0314$ for the corresponding volume concentrations (the only non-zero porosities). We assume initially that all the two-point correlation functions (determining the relative positions of the pores) are spherically symmetric; that is, we set $\alpha_{\mathrm{d}}^{(kj)}=1$ $(k,j=1,2)$. Since we are mainly interested in the effects of squirt flow, we assume that the permeability is not too high; that is, we set $\mathbf{\Gamma}=\mathbf{I}_2$ mDa. Somewhat arbitrary (but perhaps not completely unrealistic; Chapman, 2001), we write $\tau=1\mathrm{e}^{-5}$ s for the squirt flow relaxation time constant. According to Pointer et al. (2000), the viscosity of water (the saturating fluid) is 10^{-3} Pa s.

The results we have obtained for the reference medium described above are given in Fig. 1, which is composed of two subfigures. Fig. 1a shows the three complex-valued stiffness constants we have calculated as a function of frequency for the isotropic medium; only two of these are independent complex-valued parameters. [The real and imaginary parts of the stiffness coefficients are also related via Kramers–Kronig relations (e.g., Goldberger and Watson, 1964; Bourbie et al., 1987; Gross and Zhang, 1992) depending on nothing but linearity and causality, but these are not needed in the present study]. The dashed curves shows the real-valued results we have obtained by first using the T-matrix approximations for dry cavities and then using the Brown and Korringa (1975) relation to simulate the effects of fluid pressure equalization at low frequencies. The dotted curves show the real-valued results we have obtained (for the same model) by using the T-matrix approximations for fluid-saturated pores having the same stiffness tensor as water. The numerical results indicate that the T-matrix approximation used to make Fig. 1a work satisfactory in the limits of low and high frequencies. In Appendix D, it is shown analytically that an expansion of the T-matrix approximation to first order in the porosity is always consistent with the Brown–Korringa relation. Fig. 1b shows the wave speeds and attenuations we have obtained as a function of frequency from the complex-valued stiffness constants in Fig. 1a. We have used the wave equations of Carcione (1995) described in Appendix E. The results suggest that there is very little (if any) dispersion and attenuation at seismic frequencies. However, we should not forget that there is a significant amount of uncertainty associated with the squirt flow time relaxation time constant. The effect of changing the value of τ is to move the spectra along the frequency axis; the shape of the plots will however remain the same.

Fig. 2 is similar to Fig. 1, but now we have added a relatively high concentration of flat cracks that are nearly fully aligned. In addition to the parameters specified above, we took $\alpha^{(3)}=0.001$ and $\phi^{(3)}=6.2832\cdot10^{-4}$, which corresponds to a crack density of 0.15. By nearly fully aligned, we mean that the cracks are oriented in accordance with a Gaussian orientation distribution function (that is symmetric around an axis defining the zonal axis of the effective medium of hexagonal symmetry) having a standard deviation of $\pi/16$. Clearly, the T-matrix approximations still behave as expected in the limits of low and high frequency. But now there is a significant amount of dispersion and attenuation at the lower frequencies, approaching those of importance in seismic exploration and reservoir monitoring.

Fig. 3 is similar to Fig. 2, but now the standard deviation of the crack orientation distribution function is equal with $\pi/3$. Clearly, the low- and high-frequency limits as expected, but the degree of crack-induced anisotropy has diminished strongly, although the absolute values of the velocities and attenuations has been strongly affected by the weakly aligned cracks.

Fig. 4 is similar to Fig. 3, but now all crack orientation distribution functions are taken to be equally plausible, so that the crack orientation distribution function represents nothing but a normalization constant. As expected, the cracked porous medium behaves now as an isotropic viscoelastic medium. The T-matrix approximations still behaves as expected at low and high frequencies. We note that the compressional-waves are attenuated to a higher degree than the shear-waves.

Fig. 5 is similar to Fig. 4 but the two-point correlation function are no longer spherically symmetric. Specifically, we took $\alpha_{\mathrm{d}}^{(ij)}=0.5$ if $i=j$ and $\alpha_{\mathrm{d}}^{(11)}=2$ if $i\neq j$, where $i,j=1,2,3$. It is perhaps surprising that the results in Fig. 5 are consistent with the Brown–Korringa relation, despite the fact that we have relaxed on the assumption that the spatially distribution of cracks is the same for all crack pairs. [It may be noted that we have actually observed small deviations from

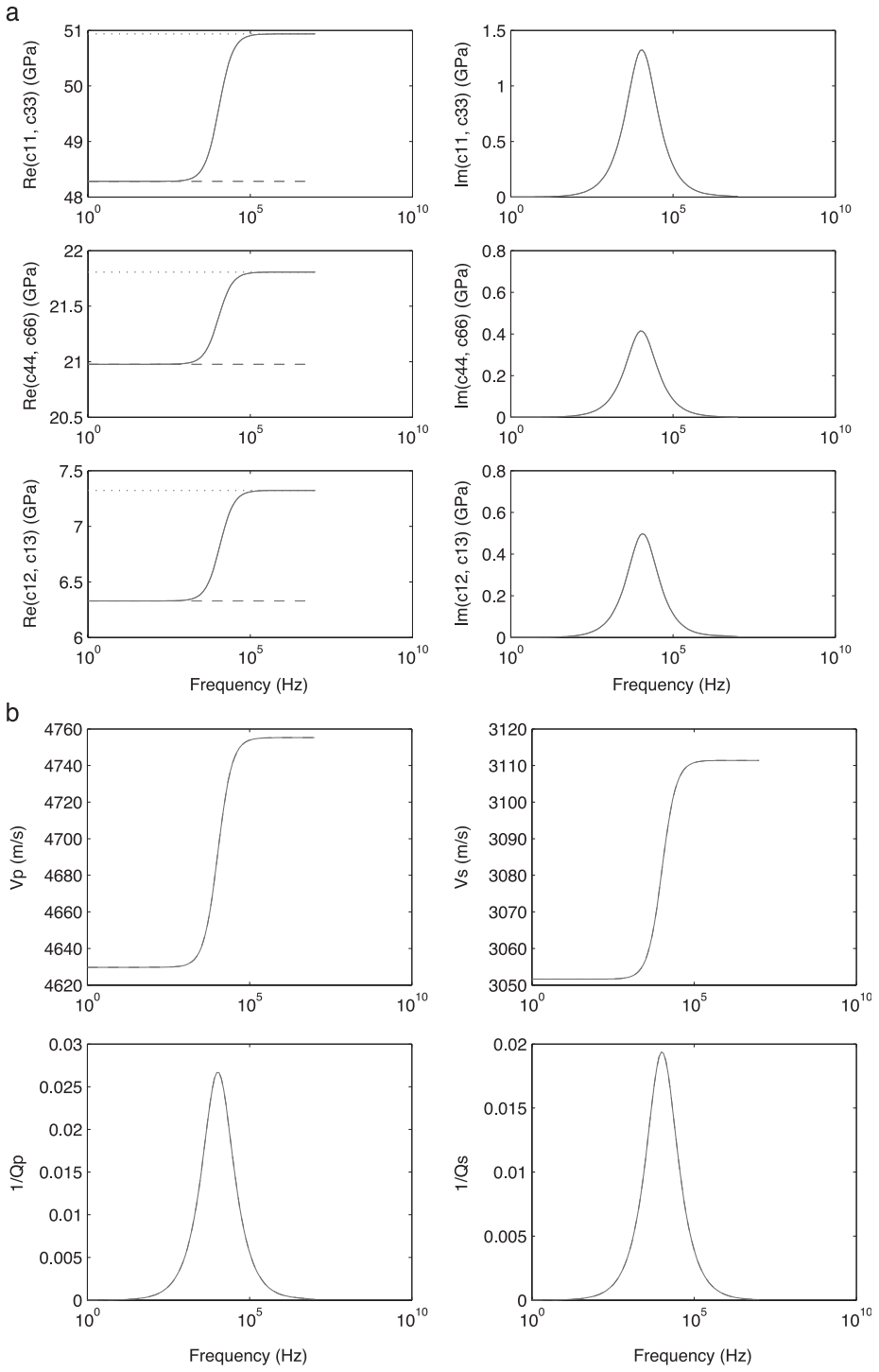
a
Re(c11, c33) (GPa)
Im(c11, c33) (GPa)
Re(c44, c66) (GPa)
Im(c44, c66) (GPa)
Re(c12, c13) (GPa)
Im(c12, c13) (GPa)
Frequency (Hz)
Frequency (Hz)
b
Vp (m/s)
Vs (m/s)
1/Qp
1/Qs
Frequency (Hz)
Frequency (Hz)

the dashed Brown–Korringa lines in other models where the spatial distributions of cavities are different for different pairs of interacting cavities, but not at small volume concentrations. We all agree that a good theory for the macroscopic properties of anisotropic porous/permeable media should be consistent with the Brown–Korringa relation, when the frequency is sufficiently low. The problem is to develop an inclusions-based model that does not only satisfy this requirement but is also valid at finite concentrations of communicating cavities (see Thomsen, 1985). When the volume concentration of inclusions increases, the phenomenon of strain propagation between different inclusions becomes increasingly important (see Gubernatis and Krumhansl, 1975; Jakobsen et al., 2003). In our theory, the fluid-saturated cavities can interact both via strain propagation and fluid flow. It appears to be difficult to show analytically that the higher-order T-matrix approximations (that takes into account strain propagation between communicating cavities) are consistent with the Brown–Korringa relation. It is only for the first-order T-matrix approximations (that ignores strain propagation between communicating cavities) that we are able to demonstrate the consistency with Brown and Korringa analytically, as shown in Appendix D.] Taking into account all the papers that have been published in this field, Fig. 5 appears to be unique in showing that crack-induced wave-speed and attenuation anisotropy may occur even if all the cracks orientations are equally plausible, provided that the spatial distribution of cracks is statistically anisotropic.

The above results were obtained for a relatively high-porosity medium containing a single set of cracks. However, we can easily extend the model to include several sets of cracks, each crack set being characterized by its own shape factor and orientation distribution function. A comparison of Figs. 3, 4 and 5 suggests that it may be difficult to tell from measurements of seismic anisotropy if it is some of the crack orientation distribution functions that lacks spherical symmetry or some of the two-point correlation functions. If all crack orientations are initially equally plausible, then the effect of an applied anisotropic stress field may not only be to (change the shapes of the cracks and) break the spherical symmetry of the crack orientation distribution function (see Tod, 2002), but also to change the symmetries of the two-point correlation functions (see Ponte Castaneda and Zaidman, 1994). Thus, there are plenty of rooms for more work along this line.

A viscoelastic medium of hexagonal symmetry is not fully characterized by the principal wave speeds and attenuations. We have therefore included an example showing the full slowness and attenuation surfaces for such a medium at a fixed frequency. The results shown in Fig. 6 were obtained by first picking the complex-valued stiffness constants corresponding with a frequency of $1.2519 \cdot 10^4$ Hz from Fig. 2 (associated with a dual porosity medium containing nearly fully aligned cracks) and then using the wave equations discussed in Appendix E. It is interesting to note that the symmetry of the medium is more strongly reflected in the attenuation surface than in the slowness surface. [Carcione et al. (1998a) also found that the attenuation is more anisotropic than the slowness, but they did not have a physical model for the medium.]

4.2. Clayey sandstones as viscoelastic composites

Sandstone reservoirs account for nearly 60% of oil reserves. In general, sandstones contain clay, which significantly affect their acoustic properties. Most previous attempts to develop effective medium models for clayey sandstones have focused on the wave speeds (e.g., Xu and White, 1995; Sams and Andrea, 2001) and ignored the attenuations. This situation should definitely change since seismic attenuation is a potentially useful parameter for characterizing and monitoring hydrocarbon reservoirs in conjunction with seismic velocity (see Klimentos and McCann, 1990; Samec and Blangy, 1992; Carcione et al., 1998b; Koesoemadinata and McMechan, 2001).

Fig. 1. The isotropic viscoelastic properties of the uncracked reference medium we use when studying the phenomenon of crack-induced anisotropy from a modern perspective. A matrix material of quartz is here containing two sets of communicating pores. The first set consists of spherical pores; the second set consists of (randomly oriented) flat pores. Dashed curves refer to the Brown–Korringa relation. Dotted curves refer to the model where the cavities are completely saturated with fluid (water in this case) but isolated with respect to fluid flow. Frequency means $\omega/(2\pi)$. (a) Frequency-dependent and complex-valued effective stiffness constants. (b) Principal wave-speed and attenuation spectra.

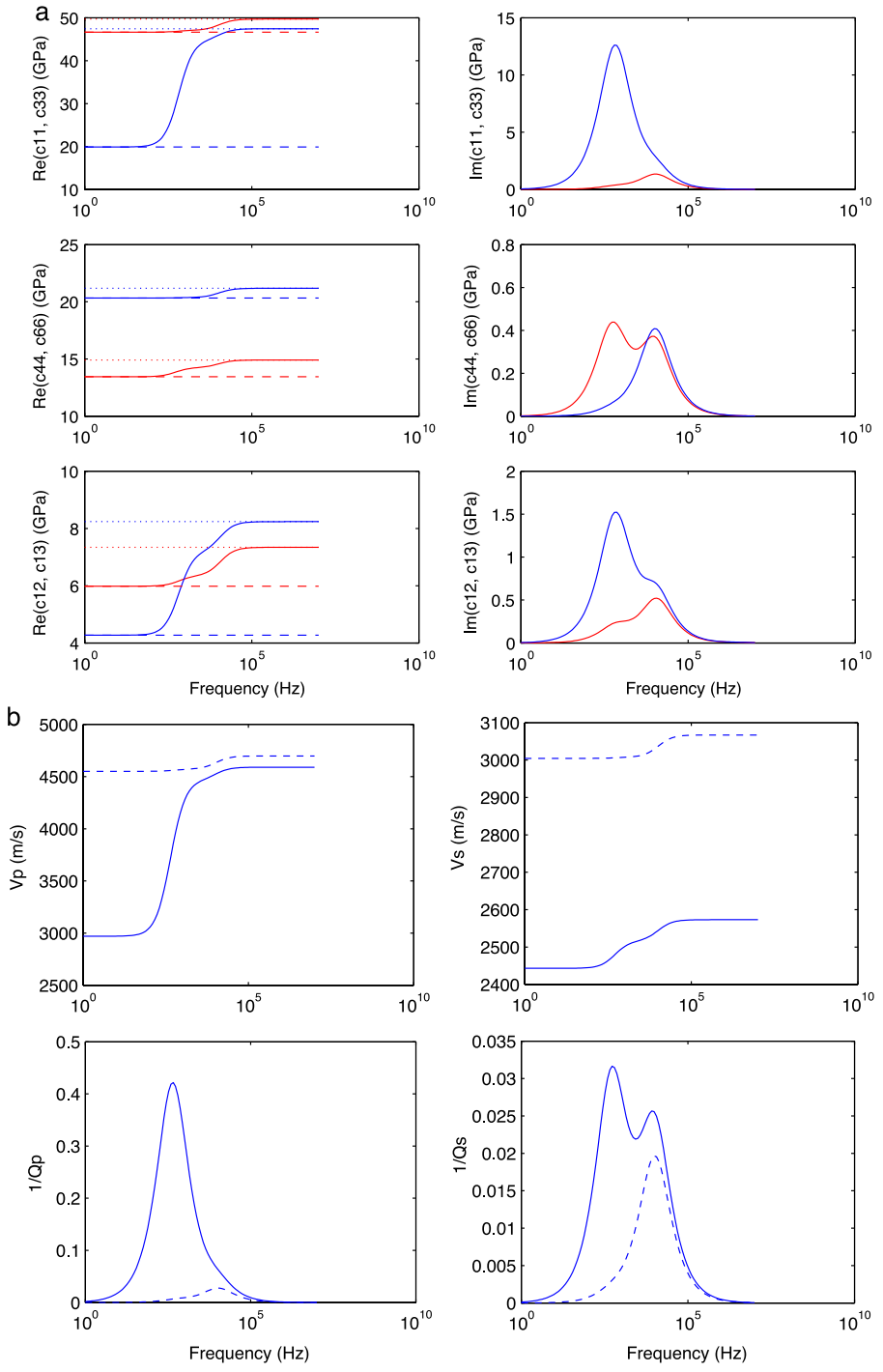

Fig. 2. The effect of nearly fully aligned cracks. The same as in Fig. 1, apart from the cracks. The red and blue curves refer to c_{11}, c_{44}, c_{12} and c_{33}, c_{66}, c_{13}, respectively.

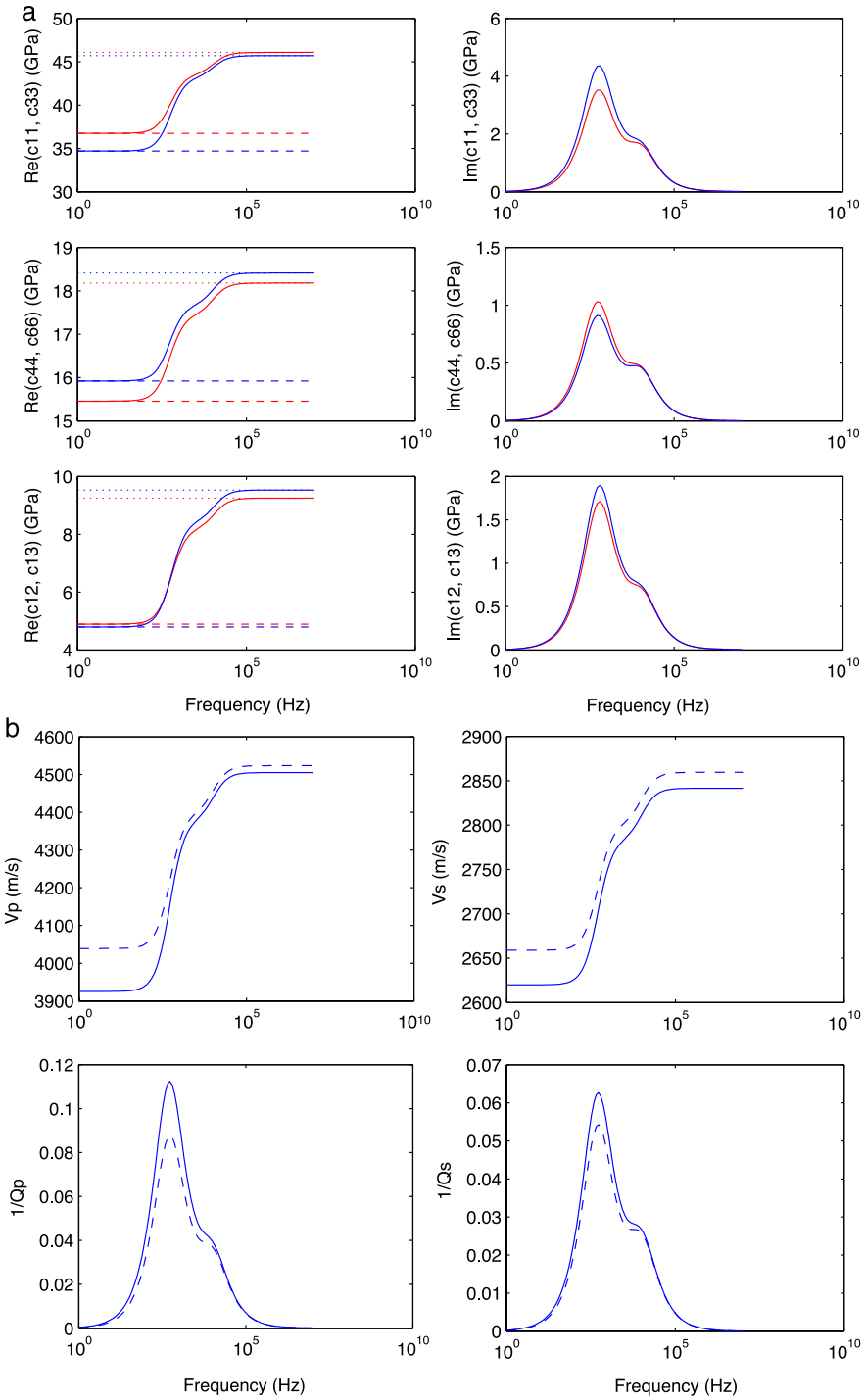

Fig. 3. The effect of weakly aligned cracks. Nearly the same as in Fig. 2, but for a wider distribution of crack orientations.

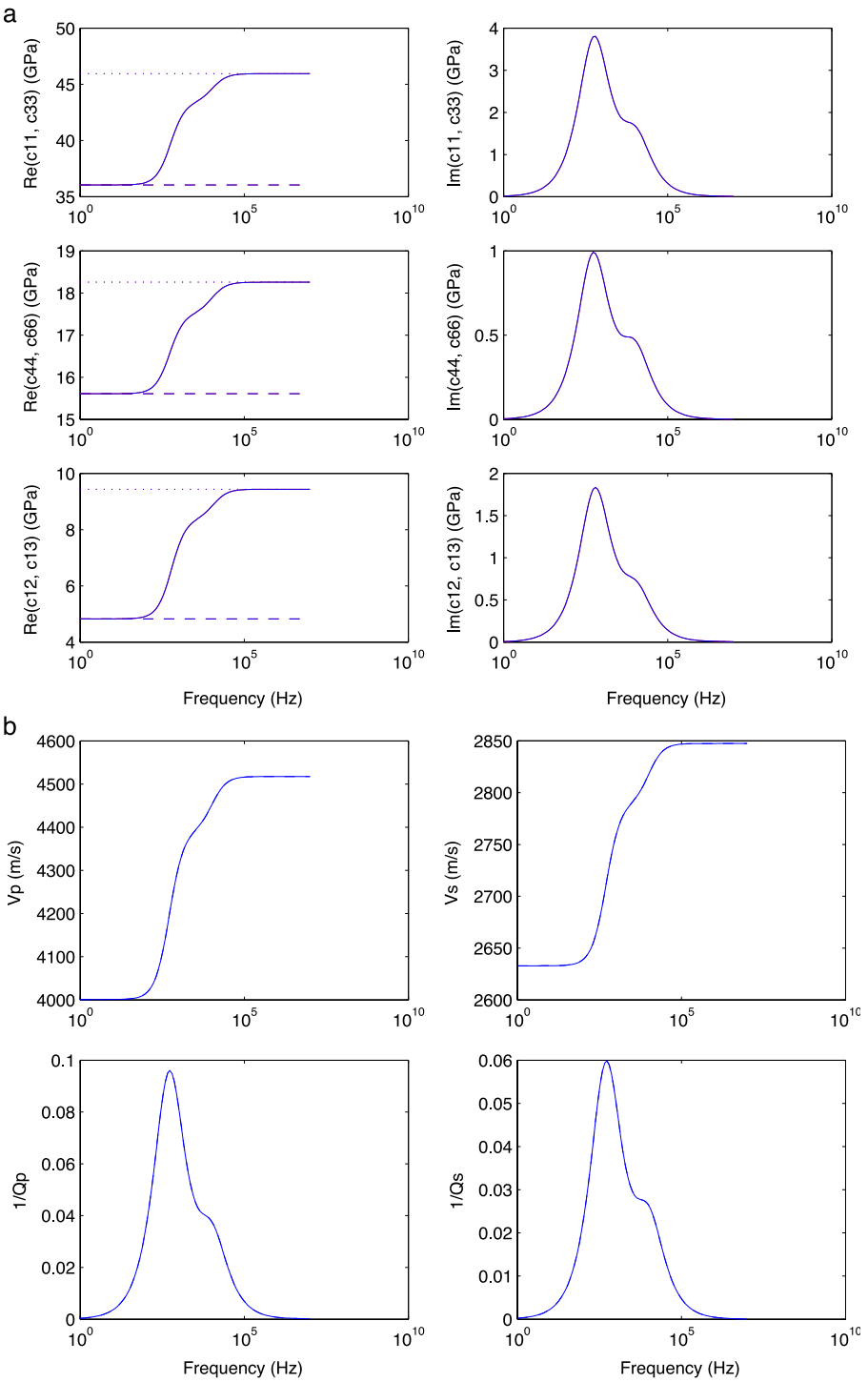

Fig. 4. The effect of cracks that are not aligned. Nearly the same as in Fig. 3, but all crack orientations are now equally plausible.

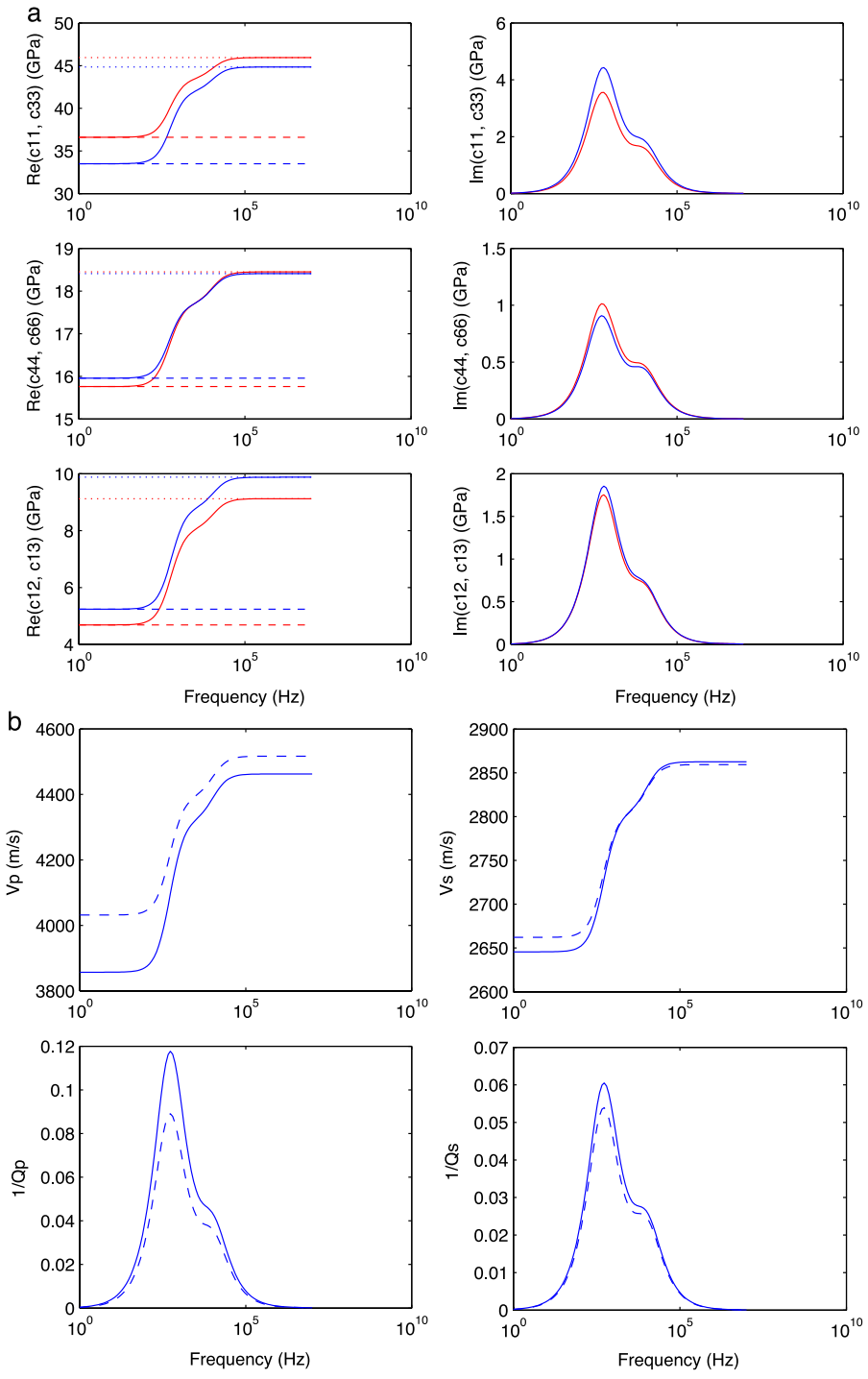

Fig. 5. The effect of spatial distribution. Nearly the same as in Fig. 4, but now the two-point correlation functions are no longer spherically symmetric and not even the same for all pairs of interacting cavities.

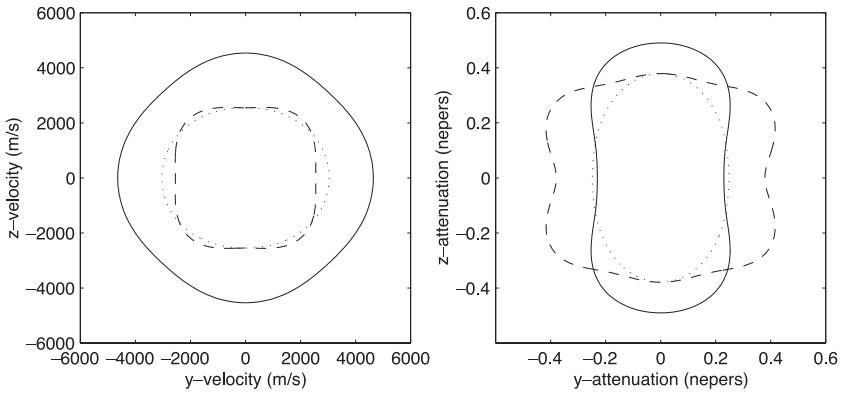

Fig. 6. Viscoelastic plane wave characteristics. We can here see the slowness and attenuation surfaces of the medium of hexagonal symmetry associated with Fig. 2 at a fixed frequency of $1.2519 \cdot 10^4$ Hz. The dotted, solid and dashed curves refer to the SH, qP and qSV modes, respectively.

The few attempts that have been made to take fluid dynamics into account (e.g., Klimentos and McCann, 1990; Carcione et al., 2000) have generally been based on the pioneering work of Biot (1956a,b), which require the dry rock properties as input. While dry rock properties can easily be measured in the

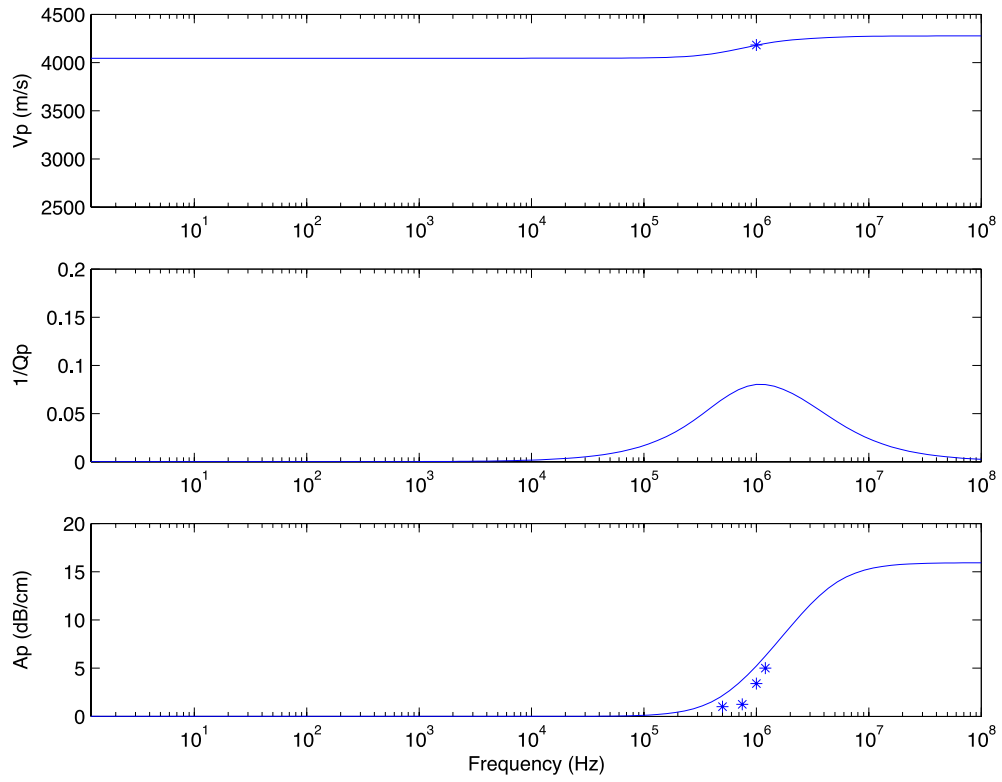

Fig. 7. Compressional wave speed and attenuation spectra for clayey sandstone sample A4BP. Solid curves are theoretical predictions; stars are experimental observations obtained under high confining pressure (40 MPa, simulated reservoir pressure conditions) with microcracks closed.

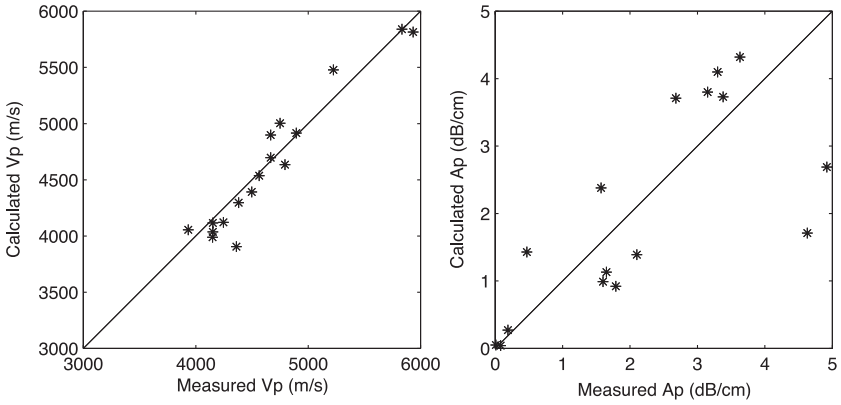

Fig. 8. Theory vs. experiment in our treatment of clayey sandstones as viscoelastic composites. We here model compressional wave speeds and attenuations at 1 MHz for a suite of clayey sandstones having porosities and clay contents (smaller than 18% and 15%) within the assumed range of our theory. The pressure condition is similar to that in Fig. 7.

laboratory, these are not practically measureable when constructing seismic models from well logs (Xu, 1998). As stated in the introduction, it is not clear if a good theory for real rocks needs to be based on the approach of Biot. After all, Klimentos and McCann (1988) have demonstrated that the slow P-wave quickly disappear when a sandstone is filled with intrapore clay. Due to the complexity of these porous media, we suggest one should try to model clayey sandstones as viscoelastic composites.

When developing inclusion-based models for clayey sandstones that takes fluid dynamics into account, it may be a good idea to use the microstructure implied by one of the more established static approaches as a starting point. According to Goldberg and Gurevich (1998), the most physically sound static approaches assume that the presence of clay in a sandstone manifests itself by the presence of pores with a low aspect ratio. The velocity model for clay-sand mixtures introduced by Xu and White

Table 2
Petrographic and compressional wave data for complex porous media of interest to the petroleum industry

Sample	Porosity (%)	Permeability (mD)	Clay content (%)	V_p^{obs} (m/s)	V_p^{calc} (m/s)	A_p^{obs} (dB/cm)	A_p^{calc} (dB/cm)
2V2M1	15.46	0.05	15.0	4152	4116	3.15	3.8
2H2M1	2.72	0.00	0	5934	5815	0.01	0.05
2V1M1	2.43	0.00	0	5835	5840	0.08	0.04
8VM1	9.96	0.01	7	4705	5003	1.79	0.92
9HM1	13.47	0.06	14	4498	4392	4.92	2.69
9VM1	17.18	0.13	15	4362	3905	6.83	4.74
9V2M1	16.71	0.44	8	4381	4296	1.57	2.38
33HM1	17.13	2.21	12	3933	4055	2.68	3.71
A1BP	16.50	41.74	15	4149	3989	3.63	4.32
A4BP	16.11	50.51	15	4152	4037	3.30	4.10
A6BP	15.41	52.42	15	4246	4122	3.38	3.73
3H1S1	13.11	3.67	7	4666	4697	2.10	1.39
3H2S1	15.72	87.55	5	4564	4536	0.47	1.43
11H2S1	15.13	11.06	4	4794	4635	1.65	1.13
14HS1	11.39	0.46	6	4666	4898	1.60	0.99
14H2S1	5.98	0.00	3	5225	5478	0.19	0.27
15HS1	10.22	0.16	9	4895	4916	4.63	1.71

We compare observed (obs) and calculated (calc) P-wave characteristics for clayey sandstones. The acoustic measurements were performed at ultrasonic frequencies under simulated reservoir pressure conditions (40 MPa confining pressure), by Klimentos and McCann (1990).

(1995) is particularly attractive, because it only complicates things up to a point, but may nevertheless capture the most essential physics involved. In this model, the total pore space is assumed to consist of two parts: (1) pores associated with quartz grains and (2) pores associated with clays. The essential feature of the model is the assumption that the clay-related pores are significantly flatter than the quartz-related pores. This makes sense since the clay minerals are much flatter than the quartz grains (see Hornby et al., 1994). The model of Xu and White (1995) ignores the effect of clay distribution on the elastic properties of sandstones. On one hand, this looks like a serious drawback since the various clay distributions may result in markedly different elastic properties (see Sams and Andrea, 2001). On the other hand, the exact location of clay particles within a sandstone is normally unknown, and the effect of averaging over a set of equally plausible distributions may be to bring the more sophisticated models of Sams and Andrea (2001) closer to the simple one of Xu and White (1995).

Since the goal of this section is merely to provide some examples of the flexibility and potential power of the T-matrix approach to rock physics, we shall assume that the microstructures of clayey sandstones are more or less as simple as suggested by Xu and White (1995). In an attempt to model the data of Klimentos and McCann (1990), three types of inclusions were embedded in a homogeneous matrix of quartz. The first type of inclusions represents the anisotropic clay minerals. We then have the quartz-related pores ($\alpha^{(1)} \approx 0.15$) and the clay-related pores ($\alpha^{(2)} \approx 0.05$). Following Xu and White (1995), we assumed that the relative proportion of clay-related pores is proportional with the clay-content. By trial and error, we have found that when the squirt flow time relaxation constant τ is equal to 10^{-7} s or so, we obtain more or less the same kind of velocity and attenuation spectra as recovered from ultrasonic laboratory data by Klimentos and McCann (1990).

Fig. 7 shows that the dual-porosity model for clayey sandstones implies a rather narrow attenuation spectrum. We here took $\alpha^{(2)} = 0.027$. With the present value of τ, the attenuation peak is in the MHz range, with no attenuation at seismic frequencies. As stated earlier, we can move the attenuation spectrum along the frequency axis (without changing its shape) simply by changing the value of the (poorly known) parameter τ. The results from the previous subsection on crack-induced anisotropy suggest that the effect of using a broader spectrum of pore shape aspect ratios is to broaden the attenuation spectrum, and so clay-related squirt flow may nevertheless be relevant for seismic exploration, depending on number of flat cavities within these materials.

Fig. 8 shows the results from a rather successful attempt to match the ultrasonic P-wave velocities and attenuations measured at a frequency of 1 MHz on the rocks in Table 2 on the basis of the above dual porosity model. The mechanical properties we have assumed for the various rock components are shown in Table 1. The agreement is seen to be more than adequate for the wave speeds and reasonable for the attenuations. What is needed (from the experimentalists) to obtain further progress is a more detailed quantitative information about the pore shape spectra of real rocks.

5. Conclusion

The T-matrix approach of standard many-body theory allows us to include the effects of intercavity fluid flow when calculating the overall properties of rock-like composites involving multiple solid constituents and cavities having all sorts of shapes, orientations, number densities and spatial distributions. It produces results that are consistent with the Brown–Korringa relation at low frequencies. Therefore, we believe that we are on the right track towards a unified theory of rocks as viscoelastic composites. The method and code we have developed may lead to a better ability to predict petrophysical properties (including the permeability) from remote seismic measurements (including the attenuation).

Acknowledgements

This paper represents some of the results that were obtained during a 1-year visit by Jakobsen to the Department of Applied Mathematics and Theoretical Physics (DAMTP) of the University of Cambridge

(UK) and a 3-month visit to the Postgraduate Research Institute for Sedimentology (PRIS) of the University of Reading (UK). Jakobsen would like to thank the staff at these institutions for providing stimulating working environments. In particular, he would like to thank Dr. John A. Hudson at DAMTP for valuable discussions.

Jakobsen would like to thank the Norwegian Research Council for awarding him the postdoctoral fellowship that made this work possible. The research of Jakobsen and Johansen has traditionally been done (and are now fully done) within the framework of the Seismic Reservoir Characterization Project at the University of Bergen. The sponsors of the SRC project (Enterprise Oil, Norsk Hydro, Statoil, Petroleum Geo-Services) are thanked for their continuing economic support.

Finally, we would like to thank the reviewers (Drs. Chapman and Carcione) for their suggestions that lead to a minor revision of the original manuscript.

Appendix A. The Kelvin notation

The Kelvin notation (e.g., Helbig, 1994; Nowick, 1995) represents an isomorphism between the tensor and matrix components that can be explained as follows. First, for a given tensor $\{A_{ijkl}\}$, pairs of indices ij and kl are converted to single indices α and β by the standard convention $11 \rightarrow 1$, $22 \rightarrow 2$, $33 \rightarrow 3$, $23, 32, \rightarrow 4$, $13, 31, \rightarrow 5$, $12, 21, \rightarrow 6$. Next, each tensor element A_{ijkl} is associated with a matrix element $A_{\alpha\beta}$ by the rules

$$A_{ijkl} = A_{\alpha\beta}, \qquad \alpha, \beta \leq 3, \tag{A-1}$$

$$A_{ijkl} = \sqrt{2}A_{\alpha\beta}, \qquad \alpha \text{ or } \beta > 3, \tag{A-2}$$

$$A_{ijkl} = 2A_{\alpha\beta}, \qquad \alpha, \beta > 3. \tag{A-3}$$

The resulting (Kelvin) matrices are of rank 6. If we use the Kelvin notation rather than the Voigt notation, all operations with the 6×6 matrices can be performed according to the usual matrix rules.

Appendix B. Effective medium approximations based on the average t-matrix

If we assume that the distribution of inclusions is the same for all inclusions pairs, in the sense that $\mathbf{G}_{\mathrm{d}}^{(rs)} = \mathbf{G}_{\mathrm{d}}$ for all r and s, then Eq. (1) reduces to

$$\mathbf{C}^{*} = \mathbf{C}^{(0)} + \mathbf{C}_1 : (\mathbf{I}_4 + \mathbf{G}_{\mathrm{d}} : \mathbf{C}_1)^{-1}, \tag{B-1}$$

which implies that

$$\mathbf{C}^{(0)} + \mathbf{C}_1 - \mathbf{C}_1 : \mathbf{G}_{\mathrm{d}} : \mathbf{C}_1 + O[(v^{(r)})^3], \tag{B-2}$$

or

$$\mathbf{C}^{*} = \mathbf{C}^{(0)} + \mathbf{C}_1 - O[(v^{(r)})^2]. \tag{B-3}$$

Recall that $\mathbf{C}^{(0)}$ can be selected rather arbitrarily. If we for a moment assume that $\mathbf{C}^{(0)}$ is the tensor of elastic constants for a matrix phase, which contains all the other phases as inclusions, then the estimate (B-1) reduces to that developed recently by Ponte Castaneda and Willis (1995); the estimate (B-2) reduces to something new, which in fact includes all the theories (or crack models) of Hudson (1980, 1981, 1994a,b) as special cases; and the estimate (B-3) agrees with the dilute result Eshelby (1957).

Since it has been written that the assumption of an infinitesimally small aspect ratio in the crack model of Hudson (1980, 1981) (which forms the basis for the works of Hudson et al., 1996; Pointer et al., 2000; Tod, 2001, 2002) is a major drawback that should not exist in future models (see Douma, 1988), let us emphasize that such an assumption does not exist in the present models.

The numerical results of Cheng (1993) and Jakobsen et al. (2002) suggest that the first-order approximation (Eq. (B-3)) and the second-order approximation (Eq. (B-2)) will become invalid as soon as the crack density (porosity) increases beyond 0.1 (10%) or so. This is an unfortunate feature since rocks of interest to the petroleum industry frequently has crack densities (porosities) as high as 0.3 (40%) or even higher (see Thomsen, 1995). The first- and second-order approximations may not be suitable for

dealing with multiple solid constituents either, particularly not with mixtures of rounded quartz minerals and flat anisotropic clay minerals (see Jakobsen et al., 2003).

In many applications, it may be a good idea to use the general T-matrix approximation (Eq. (1)) or its simplified version (Eq. (B-1)). The fact that these approximations contain terms of all orders in the volume concentrations of inclusions gives us a limited encouragement to proceed with their application in circumstances where the first- and second-order approximations completely fail. More encouragement is provided by the analytical and numerical results of Jakobsen et al. (2003). Ponte Castaneda and Willis (1995) have shown that one can find the highest possible inclusion concentration where the simplified approximation (Eq. (B-1)) is strictly valid if we know the shape of the inclusions and their spatial distribution. For the special case of a homogeneous matrix material containing just one type of inclusions, the maximum possible value for the aspect ratio α_d of the correlation function for given aspect ratio $\alpha^{(2)}$ and volume concentration $v^{(2)}$ of the inclusions (phase 2) is (given by Ponte Castaneda and Willis, 1995) $\alpha|_{\min} = \alpha_d v^{(2)}$, and correspondingly the maximum possible value of α_d for given $\alpha^{(2)}$ and $v^{(2)}$ is $\alpha\,|_{\max} = \alpha^{(2)}/v^{(2)}$.

Appendix C. Evaluation of the G tensor

Jakobsen et al. (2003) show that

$$G^{(r)}_{pqrs} = -\frac{1}{4}\left(E^{(r)}_{pqrs} + E^{(r)}_{pqsr} + E^{(r)}_{qprs} + E^{(r)}_{qpsr}\right), \quad (C-1)$$

where

$$E^{(r)}_{pqrs} = \int_0^{\pi} d\theta \sin\theta \int_0^{2\pi} d\phi D^{-1}_{qs}(\mathbf{k}) k_p k_r A^{(r)}(\theta,\phi), \quad (C-2)$$

and $D^{-1}_{pr}(\mathbf{k})$ is the inverse matrix of the Fourier transform of the displacement Green's function, and

$$A^{(r)}(\theta,\phi) = \frac{1}{\pi\,|\,\Omega^{(r)}\,|}\int_0^{\infty} dk k^2 \int_{\Omega^{(r)}} dx e^{-i\mathbf{k}\cdot\mathbf{x}} \times \int_{\Omega^{(r)}} dx' e^{i\mathbf{k}\cdot\mathbf{x}'}, \quad (C-3)$$

where k, θ and ϕ are the spherical coordinates in $\mathbf{k}$ space, and k_i the Cartesian components of $\mathbf{k}$. Obviously, $A^{(r)}$ represent a shape/orientation factor independent of the elastic constants. For a sphere, $A^{(r)} = 1/4\pi$ and $\mathbf{G}^{(r)}$ becomes identical with the χ tensor, which is associated with crack–crack interactions in Hudson's crack model. For an oblate spheriodal inclusion, the purely geometric factor is given by (Jakobsen et al., submitted for publication)

$$A^{(r)}(\theta) = \frac{1}{4\pi}\frac{b_1^2 b_3}{\left[b_1^2\sin^2\theta + b_3^2\cos^2\theta\right]^{3/2}}. \quad (C-4)$$

Further progress along this line may now easily be obtained by first combining Eqs. (C-2) and (C-4), and then solve the resulting integrals by using symbolic and/or numerical methods. For other treatments and, partially, more general theorems of the inclusion problem, see Ponte Castaneda and Willis (1995), Kroner (1986, p. 262) and Mura (1982). The tensor $\mathbf{G}^{(r)}$ is simply given by $-\mathbf{P}^{(r)}$, where $\mathbf{P}^{(r)}$ is a tensor well known for the works of Willis and his associates. Mura (1982) gives expressions for the $\mathbf{G}^{(r)}$ tensors for all sorts of inclusions, including cracks in isotropic and anisotropic media.

Appendix D. The low-frequency limit

Brown and Korringa (1975) derived an expression for the saturated (undrained) compliances in terms of the dry result;

$$S^*_{ijkl} = S^d_{ijkl} + \frac{\left(S^*_d - S^{(0)}\right)_{ijuu}\left(S^*_d - S^{(0)}\right)_{vvkl}}{\phi^0\left(S^{(0)}_{uuvv} - 1/\kappa_f\right) - \left(S^*_d - S^{(0)}\right)_{uuvv}}, \quad (D-1)$$

where $\phi^0 = \sum_{j=1}^{J_c}\phi^{(j)}$ is the total porosity. The relation (D-1) was derived from the following equation:

$$\mathbf{S}^* : \boldsymbol{\sigma}^{(0)} = \mathbf{S}^*_d : \left(\boldsymbol{\sigma}^{(0)} + \mathbf{I}_2 p_f\right) - \mathbf{S}^{(0)} : \mathbf{I}_2 p_f, \quad (D-2)$$

which has the same structure as Eq. (11).

Although the above relations were derived from first principles, Brown and Korringa (1975) did not use a specific model for the porous microstructure but

assumed the frequency to be sufficiently low so that the pore fluid pressure is equilibrated throughout the pore space. It is now clear that this may or may not be a good approximation at seismic frequencies, depending on the geometry of the porous microstructure.

As pointed out by Xu (1998), both Eqs. (D-1) and (D-2) represent a generalization of Gassmann's (1951) famous relation for isotropic porous media, and can be used to check if an inclusion-based theory for the effective stiffnesses of an anisotropic porous media have the correct dependence on the elastic properties of the saturating fluid at low frequencies. In this appendix, we shall investigate if the first-order approximation (Eq. (B-3)) is consistent with the following equation:

$$\mathbf{S}^* = \mathbf{S}^*_{\mathrm{d}} + (\mathbf{S}^*_{\mathrm{d}} - \mathbf{S}^{(0)}) : (\mathbf{I}_2 \otimes \psi), \qquad (\mathrm{D}-3)$$

which follows from Eqs. (D-2) and (26), in conjunction with the fact that $\boldsymbol{\sigma}^{(0)}$ is arbitrary.

From Eq. (B-3), we get

$$\begin{aligned}
\mathbf{S}^* &\approx (\mathbf{C}^{(0)} + \mathbf{C}_1)^{-1}, \\
&= [(\mathbf{I}_4 + \mathbf{C}_1 : \mathbf{S}^{(0)}) : \mathbf{C}^{(0)}]^{-1}, \\
&= \mathbf{S}^{(0)} : (\mathbf{I}_4 + \mathbf{C}_1 : \mathbf{S}^{(0)})^{-1}, \\
&\approx \mathbf{S}^{(0)} : (\mathbf{I}_4 - \mathbf{C}_1 : \mathbf{S}^{(0)}), \\
&= \mathbf{S}^{(0)} - \mathbf{S}^{(0)} : \mathbf{C}_1 : \mathbf{S}^{(0)}. \qquad (\mathrm{D}-4)
\end{aligned}$$

From Eqs. (2) and (19), we get

$$\mathbf{C}_1 = \mathbf{C}_1^d + \mathbf{C}_1^f, \qquad (\mathrm{D}-5)$$

where

$$\mathbf{C}_1^d = \sum_r v^{(r)} \mathbf{t}_{\mathrm{d}}^{(r)} \qquad (\mathrm{D}-6)$$

and

$$\mathbf{C}_1^f = \sum_r v^{(r)} \mathbf{t}_{\mathrm{d}}^{(r)} : \mathbf{S}^{(0)} : (\mathbf{I}_2 \otimes \psi^{(n)}) : \mathbf{C}^{(0)}. \qquad (\mathrm{D}-7)$$

Eqs. (D-4) and (D-5) imply that

$$\mathbf{S}^* \approx \mathbf{S}^*_{\mathrm{d}} - \mathbf{S}^{(0)} : \mathbf{C}_1^f : \mathbf{S}^{(0)}, \qquad (\mathrm{D}-8)$$

where

$$\mathbf{S}^*_{\mathrm{d}} = \mathbf{S}^{(0)} - \mathbf{S}^{(0)} : \mathbf{C}_1^d : \mathbf{S}^{(0)}. \qquad (\mathrm{D}-9)$$

From Eq. (27), it is clear that

$$\lim_{\omega \to 0} \psi^{(n)} = \psi. \qquad (\mathrm{D}-10)$$

Eqs. (D-6), (D-7) and (D-10) give

$$\lim_{\omega \to 0} \mathbf{C}_1^f = \mathbf{C}_1^d : \mathbf{S}^{(0)} : (\mathbf{I}_2 \otimes \psi) : \mathbf{C}^{(0)}. \qquad (\mathrm{D}-11)$$

It follows from Eqs. (D-8) and (D-11) that

$$\lim_{\omega \to 0} \mathbf{S}^* \approx \mathbf{S}^*_{\mathrm{d}} - \mathbf{S}^{(0)} : \mathbf{C}_1^d : \mathbf{S}^{(0)} : (\mathbf{I}_2 \otimes \psi). \qquad (\mathrm{D}-12)$$

Eqs. (D-12) and (D-9) imply that

$$\lim_{\omega \to 0} \mathbf{S}^* \approx \mathbf{S}^*_{\mathrm{d}} + (\mathbf{S}^*_{\mathrm{d}} - \mathbf{S}^{(0)}) : (\mathbf{I}_2 \otimes \psi), \qquad (\mathrm{D}-13)$$

which agree with the Brown–Korringa relation (Eq. (D-3)).

Appendix E. Long waves in viscoelastic composites

The time-reduced equation of motion for harmonic vibrations of angular frequency ω in any continuum (not subjected to any body forces) may be given in the form

$$\nabla \cdot \boldsymbol{\sigma}(\mathbf{x}, \omega) = i\omega \mathbf{p}(\mathbf{x}, \omega), \qquad (\mathrm{E}-1)$$

where $\boldsymbol{\sigma}(\mathbf{x}, \omega)$ is the stress tensor and $\mathbf{p}(\mathbf{x}, \omega)$ is the momentum density vector. The above equation is independent of material properties. These enter through the constitutive relations for the stress, e.g.,

$$\boldsymbol{\sigma}(\mathbf{x}, \omega) = \mathbf{C}(\mathbf{x}, \omega) : \boldsymbol{\epsilon}(\mathbf{x}, \omega), \qquad (\mathrm{E}-2)$$

and the additional relation

$$\mathbf{p}(\mathbf{x}, \omega) = i\omega \rho(\mathbf{x}) \mathbf{u}(\mathbf{x}, \omega), \qquad (\mathrm{E}-3)$$

for the momentum density, where $\rho(\mathbf{x})$ is the mass density of the medium and $\mathbf{u}(\mathbf{x}, \omega)$ is its displacement. Eq. (E-2) (becomes a convolution in the time domain) is called the Boltzmann superposition principle, and represents the most general constitutive relation for an

anisotropic and linear viscoelastic medium (see Carcione, 1995).

We now assume that the local stiffness tensor $\mathbf{C}(\mathbf{x}, \omega)$ and the local density $\rho(\mathbf{x})$ vary in a random manner on a length-scale, which is small compared with all other length-scales including that associated with the wavelength of an acoustic wave. If similar relations hold for at the macroscopic scale; namely,

$$\nabla \cdot \langle \boldsymbol{\sigma}(\mathbf{x}, \omega) \rangle = i\omega \langle \mathbf{p}(\mathbf{x}, \omega) \rangle, \qquad (\mathrm{E}-4)$$

$$\langle \boldsymbol{\sigma}(\mathbf{x}, \omega) \rangle = \mathrm{C}^*(\omega) : \langle \boldsymbol{\epsilon}(\mathbf{x}, \omega) \rangle, \qquad (\mathrm{E}-5)$$

$$\langle \mathbf{p}(\mathbf{x}, \omega) \rangle = i\omega \rho^*(\omega) \langle \mathbf{u}(\mathbf{x}, \omega) \rangle, \qquad (\mathrm{E}-6)$$

then our job is to determine the effective stiffness tensor $\mathbf{C}^*(\omega)$ and the effective density $\rho^*(\omega)$, from the statistical information we have about the fluctuations in local stiffnesses and density. In the above equations, the brackets $\langle \cdot \rangle$ denote the ensemble average. If the random composite is statistically homogeneous (as we assume in the following), then $\mathbf{C}^*(\omega)$ may be estimated on the basis of a static theory of composites in conjunction with the elastic–viscoelastic correspondence principle (discussed earlier), and $\rho^*(\omega)$ is simply given by the (frequency-independent) spatially averaged density for the micro-inhomogeneous material as a whole (e.g., Willis, 1981; Hudson, 1994a).

A general solution for the mean displacement field representing viscoelastic plane waves is of the form

$$\langle \mathbf{u}(\mathbf{x}, t) \rangle = \mathbf{U} \mathrm{e}^{i(\omega t - \mathbf{k} \cdot \mathbf{x})}, \qquad (\mathrm{E}-7)$$

where $\mathbf{U}$ is a constant complex polarization vector. For homogeneous waves, the components of the wave number vector can be written as

$$\mathbf{k} = (\kappa - i\alpha)\hat{\mathbf{l}} \equiv k\hat{\mathbf{l}}, \qquad (\mathrm{E}-8)$$

where

$$\hat{\mathbf{l}} = l_i \hat{\mathbf{e}}_i, \qquad (\mathrm{E}-9)$$

defines the propagation direction through the direction cosines l_i. For a homogeneous plane wave, planes of constant phase are parallel to planes of constant amplitude. The dispersion relation is given by (Auld, 1990; Carcione, 1995)

$$\det[C^*_{ijkl}(\omega) l_j l_l - \rho^* V^2 \delta_{ik}] = 0, \qquad (\mathrm{E}-10)$$

where

$$V = \frac{\omega}{k}, \qquad (\mathrm{E}-11)$$

is the complex velocity.

Using Eq. (11), the components of the slowness and attenuation vectors can be expressed in terms of the complex velocity as (given by Carcione, 1995)

$$\mathrm{s} = Re\left[\frac{1}{V}\right]\hat{\mathbf{l}}, \qquad (\mathrm{E}-12)$$

and

$$\boldsymbol{\alpha} = -\omega Im\left[\frac{1}{V}\right]\mathbf{l}. \qquad (\mathrm{E}-13)$$

The phase velocity is the reciprocal of the slowness and is given in component form by (Carcione, 1995)

$$\mathbf{V}_p = \left(Re\left[\frac{1}{V}\right]\right)^{-1}\hat{\mathbf{l}}. \qquad (\mathrm{E}-14)$$

The quality factor Q is defined as the ratio of the peak strain energy density to the average loss energy density (Auld, 1990), and is given by (Carcione, 1995)

$$Q = \frac{Re[V^2]}{Im[V^2]}. \qquad (\mathrm{E}-15)$$

The handbook of Carcione (2001) represents an alternative reference for Eqs. (E-10) (E-11) (E-12) (E-13) (E-14) (E-15) among others.

References

Auld, B.A., 1990. Acoustic Fields and Waves in Solids. Krieger Publishing, Malabar, FL.

Berryman, J.G., 1992. Single-scattering approximations for coefficients in Biot's equations of poroelasticity. J. Acoust. Soc. Am. 91, 551–571.

Berryman, J.G., 1998. Rocks as Poroelastic Composites. Poromechanics, Thimus et al. Balkema, Rotterdam ISBN 9058090035.

Berryman, J.G., Milton, G.W., 1991. Exact results for generalized

Gassmann's equations in composite porous media with two constituents. Geophysics 56, 1950–1960.
Berryman, J.G., Wang, H.F., 1998. Elastic wave propagation and attenuation in a double-porosity dual-permeability medium. Int. J. Rock Mech. Min. Sci. Geomech. 37, 63–78.
Best, A.I., McCann, C., Sothcott, J., 1994. The relationships between velocities, attenuations and petrophysical properties of reservoir sedimentary rocks. Geophys. Prospect. 42, 151–178.
Biot, M.A., 1956a. Theory of propagation of elastic waves in a fluid saturated solid: I. Lower frequency range. J. Acoust. Soc. Am. 28, 168–178.
Biot, M.A., 1956b. Theory of propagation of elastic waves in a fluid saturated solid: II. Higher frequency range. J. Acoust. Soc. Am. 28, 179–191.
Bourbie, T., Coussy, O., Zinszner, B., 1987. Acoustics of Porous Media. Editions Technip, Paris.
Brinson, L.C., Lin, W.S., 1998. Comparison of micromechanics methods for effective properties of multiphase viscoelastic composites. Compos. Struct. 41, 353–367.
Brown, R.J.S., Korringa, J., 1975. On the dependence of elastic properties of a porous rock on the compressibility of the pore fluid. Geophysics 40, 608–616.
Budiansky, B., O'Connell, R.J., 1980. Bulk dissipation in heterogeneous media. Solid Earth Geophys. Geotech. 42, 1–10.
Burridge, R., Keller, J.B., 1981. Poroelasticity equations derived from microstructure. J. Acoust. Soc. Am. 70, 1140–1146.
Carcione, J.M., 1995. Constitutive model and wave equations for linear, viscoelastic, anisotropic media. Geophysics 60, 537–548.
Carcione, J.M., 2001. Wave fields in real media: wave propagation in anisotropic, anelastic and porous media. Handbook of Geophysical Exploration. Pergamon Press, Amsterdam.
Carcione, J.M., Cavallini, F., Helbig, K., 1998a. Anisotropic attenuation and material symmetry. Acustica 84, 495–502.
Carcione, J.M., Helle, H.B., Zhao, T., 1998b. Effects of attenuation and anisotropy on reflection amplitude versus offset. Geophysics 63, 1652–1658.
Carcione, J.M., Gurevich, B., Cavallini, F., 2000. A generalized Biot–Gassmann model for the acoustic properties of shaley sandstones. Geophys. Prospect. 48, 539–557.
Carcione, J.M., Helle, H.B., Pham, N.H., 2002. White's model for wave propagation in partially saturated rocks: comparison with poroelastic numerical experiments. Geophysics. Submitted for publication.
Chapman, M., 2001. Modelling the wide band laboratory response of rock samples to fluid and pressure changes. PhD thesis, University of Edinburgh.
Chapman, M., 2002. Frequency dependent anisotropy due to mesoscale fractures in the presence of equant porosity. Extended Abstract, 64th EAGE Conference and Technical Exhibition, Florence, Italy.
Chapman, M., Zatsepin, S.V., Crampin, S., 2002. Derivation of a microstructural poroelastic model. Submitted to Geophys. J. Int. 150, 1–25.
Cheng, C.H., 1993. Crack models for a transversely isotropic medium. J. Geophys. Res. 98, 675–684.
Cheng, C.H., Toksoz, M.N., 1979. Inversion of seismic velocities for the poreaspect ratio spectrum of a rock. J. Geophys. Res. 84, 7533–7543.
Domany, E., Gubernatis, J.E., Krumhansl, J.A., 1975. The elasticity of polycrystals and rocks. J. Geophys. Res. 80, 4851–4856.
Domnesteanu, P., McCann, C., Sothcott, J., 2002. Velocity anisotropy and attenuation of shale in under- and over pressured conditions. Geophys. Prospect. 50, 487–503.
Douma, J., 1988. The effect of the aspect ratio on cracked-induced anisotropy. Geophys. Prospect. 36, 614–632.
Dunn, M.L., 1995. Viscoelastic damping of particle and fiber reinforced composite materials. J. Acoust. Soc. Am. 98, 3360–3374.
Dvorkin, J., Nur, A., 1993. Dynamic poroelasticity: a unified model with the squirt and the Biot mechanisms. Geophysics 58, 524–533.
Endres, A.L., 1997. Geometrical models for poroelastic behaviour. Geophys. J. Int. 128, 522–532.
Endres, A.L., Knight, R.J., 1997. Incorporating pore geometry and fluid pressure communication into modelling the elastic behaviour of porous rocks. Geophysics 62, 106–117.
Eshelby, J.D., 1957. The determination of the elastic field of an ellipsoidal inclusion, and related problems. Proc. R. Soc. Lond., A 241, 376–396.
Gassmann, F., 1951. Uber die elastizitat poroser medien: vierteljahresschr. Naturforsch. Ges. Zurich 96, 1–21.
Gibiansky, L.V., Torquato, S., 1998. New method to generate three-point bounds on effective properties of composites: application to viscoelasticity. J. Mech. Phys. Solids 46, 749–783.
Goldberg, I., Gurevich, B., 1998. A semi-empirical velocity-porosity-clay model for petrophysical interpretation of P- and S-velocities. Geophys. Prospect. 46, 271–285.
Goldberger, M.L., Watson, K.M., 1964. Collision Theory. Wiley, New York.
Gross, D., Zhang, C., 1992. Wave-propagation in damaged solids. Int. J. Solids Struct. 29, 1763–1779.
Gubernatis, J.E., Krumhansl, J.A., 1975. Macroscopic engineering properties of polycrystalline materials: elastic properties. J. Appl. Phys. 46, 1875–1883.
Gurevich, B., Lopatnikov, S.L., 1995. Velocity and attenuation of elastic waves in finely layered porous rocks. Geophys. J. Int. 121, 933–947.
Helbig, K., 1994. Fundations of anisotropy for exploration seismics. Handbook of Geophysical Exploration. Pergamon Press, New York.
Hornby, B.E., Schwartz, L.M., Hudson, J.A., 1994. Anisotropic effective medium modeling of the elastic properties of shales. Geophysics 59, 1570–1583.
Hudson, J.A., 1980. Overall properties of a cracked solid. Math. Proc. Camb. Phil. Soc. 88, 371–384.
Hudson, J.A., 1981. Wave speeds and attenuation of elastic waves in material containing cracks. Geophys. J.R. Astron. Soc. 87, 265–274.
Hudson, J.A., 1994a. Overall properties of a material with inclusions or cavities. Geophys. J. Int. 117, 555–561.
Hudson, J.A., 1994b. Overall properties of anisotropic materials containing cracks. Geophys. J. Int. 116, 279–282.

Hudson, J.A., Liu, E., Crampin, S., 1996. The mechanical properties of materials with interconnected cracks and pores. Geophys. J. Int. 124, 105–112.

Hudson, J.A., Pointer, T., Liu, E., 2001. Effective medium theories for fluid saturated materials with aligned cracks. Geophys. Prospect. 49, 509–522.

Jakobsen, M., Johansen, T.A., 1999. A test of ANNIE based on ultrasonic measurements on a shale. J. Seism. Explor. 8, 77–89.

Jakobsen, M., Johansen, T.A., 2000. Anisotropic approximations for mudrocks: a seismic laboratory study. Geophysics 65, 1711–1725.

Jakobsen, M., Hudson, J.A., Minshull, T.A., Singh, S.C., 2000. Elastic properties of hydrate-bearing sediments using effective medium theory. J. Geophys. Res. 105, 561–577.

Jakobsen, M., Hudson, J.A., Johansen, T.A., 2003. T-matrix approach to shale acoustics. Submitted to Geophys. J. Int.

Jeffreys, H., Jeffreys, B.S., 1972. Methods of Mathematical Physics. Cambridge Mathematical Library, Cambridge.

Jones, T.D., 1986. Pore fluids and frequency-dependent wave propagation in rocks. Geophysics 51, 1939–1953.

Klimentos, T., McCann, C., 1988. Why is the Biot slow compressional wave not observed in real rocks? Geophysics 53, 1605–1609.

Klimentos, T., McCann, C., 1990. Relationships among compressional wave attenuation, porosity, clay content, and permeability in sandstones. Geophysics 55, 998–1014.

Koesoemadinata, A.P., McMechan, G.A., 2001. Sensitivity of viscoelastic reflection amplitude variation with angle to petrophysical properties. J. Seism. Expl. 9, 269–284.

Korringa, J., 1979. Multiple scattering theory and the self-consistent imbedding approximation. In: Varadan, V.K., Varadan, V.V. (Eds.), Acoustic, Electromagnetic and Elastic Wave Scattering-Focus on the T-Matrix Approach. Proceedings of The International Symposion Held at The Ohio State University. Pergamon Press, New York, pp. 529–535.

Kroner, E., 1986. Statistical modelling. In: Gittus, J., Zarka, J. (Eds.), Modelling Small Deformations of Polycrystals. Elsevier Applied Science, London, pp. 229–291.

McCann, C., Sothcott, J., Assefa, S.B., 1997. Prediction of petrophysical properties from seismicquality factor measurements. Developments in Petrophysics, Geological Society Special Publication 122, 121–130.

McCoy, J.J., 1979. On the calculation of bulk material properties of heterogeneous materials. Q. Appl. Math., July, 137–149.

Menke, W., Dubendorff, B., 1985. Discriminating intrinisc and apparent attenuation in layered rock. Geophys. Res. Lett. 12, 721–724.

Molinari, A., Mouden, M.E., 1996. The problem of elastic inclusions at finite concentrations. Int. J. Solids Struct. 33, 3131–3150.

Morris, P.R., 1969. Averaging fourth-rank tensors with weight functions. J. Appl. Phys. 40, 447–448.

Mukerji, T., Mavko, G., 1994. Pore fluid effects on seismic velocity in anisotropic rocks. Geophysics 59, 233–244.

Mura, T., 1982. Micromechanics of Defects in Solids. Martinus Nijhoff, Zoetermeer, Netherlands.

Nan, C.W., Birringer, R., Gleiter, H., 1998. On correlation effect in t-matrix method for effective elastic moduli of composites. Phys. Status Solidi, B Basic Res. 205, R9–R10.

Nemat-Nasser, S., Hori, M., 1993. Micromechanics: overall properties of heterogeneous materials. Appl. Math. Mech., vol. 37. North-Holland, New York.

Nowick, S.A., 1995. Crystal Properties Via Group Theory. Cambridge University Press, Cambridge.

O'Connell, R., 1983. A viscoelastic model of anelasticity of fluid saturated porous rocks. In: Johnson, D.L., Sen, P.N. (Eds.), Physics and Chemistry of Porous Media. Schlumberger-Doll Research. AIP Conference Proceedings, American Institute of Physics, New York, pp. 166–175.

O'Connell, R., Budiansky, B., 1977. Viscoelastic properties of fluid-saturated cracked solids. J. Geophys. Res. 82, 5719–5735.

Pointer, T., Liu, E., Hudson, J.A., 2000. Seismic wave propagation in cracked porous media. Geophys. J. Int. 142, 199–231.

Ponte Castaneda, P., Willis, J.R., 1995. The effect of spatial distribution on the effectivebehaviour of composite materials and cracked media. J. Mech. Phys. Solids 43, 1919–1951.

Ponte Castaneda, P., Zaidman, M., 1994. Constitutive models for porous materials with evolving microstructure. J. Mech. Phys. Solids 42, 1459–1497.

Ravalec, M.L., Gueguen, Y., 1996. High- and low-frequency elastic moduli for a saturated porous/cracked rock-differential self-consistent and poroelastictheories. Geophysics 61, 1080–1094.

Sams, M.S., Andrea, M., 2001. The effect of clay distribution on the elastic properties ofsandstones. Geophys. Prospect. 49, 128–150.

Samec, P., Blangy, J.P., 1992. Viscoelastic attenuation, anisotropy, and AVO. Geophysics 57, 441–450.

Sayers, C.M., 1994. The elastic anisotropy of shales. J. Geophys. Res. 99, 767–774.

Shafiro, B., Kachanov, M., 1997. Materials with fluid-filled pores of various shapes: effective elastic propertiesand fluid pressure polarization. Int. J. Solids Struct. 34, 3517–3540.

Thomsen, L., 1985. Biot-consistent elastic moduli of porous rocks: low frequency limit. Geophysics 50, 2797–2807.

Thomsen, L., 1995. Elastic anisotropy due to aligned cracksin porous rock. Geophys. Prospect. 43, 805–829.

Tittmann, B.R., 1977. Lunar rock Q in 3000–5000 range achieved in the laboratory. Philos. Trans. R. Soc. Am. 285, 475–479.

Tod, S., 2001. Effects on seismic waves of nearly aligned cracks. Geophys. J. Int. 146, 249–263.

Tod, S.R., 2002. The effects of stress and fluid pressure on the anisotropy of interconnected cracks. Geophys. J. Int. 149, 149–156.

Willis, J.R., 1981. Variational and related methodsfor the overall properties of composites. Adv. Appl. Mech. 21, 1–78.

Xu, S., White, R.E., 1995. A new velocity model for clay–sand mixtures. Geophys. Prospect. 43, 91–118.

Xu, S., 1998. Modelling the effect of fluid communicationon velocities in anisotropic porous rocks. Int. J. Solids Struct. 35, 4685–4707.

Zeller, R., Dederich, P.H., 1973. Elastic constants of polycrystals. Phys. Status Solidi, B Basic Res. 55, 831–843.